Journal of Proteomics 191 (2019) 212–227

Contents lists available at ScienceDirect

Journal of Proteomics

journal homepage: www.elsevier.com/locate/jprot

Proteomic analysis of the sarcolemma-enriched fraction from dystrophic *mdx-4cv* skeletal muscle

Sandra Murphy[a], Margit Zweyer[b], Michael Henry[c], Paula Meleady[c], Rustam R. Mundegar[b], Dieter Swandulla[b], Kay Ohlendieck[a,*]

[a] Department of Biology, Maynooth University, National University of Ireland, Maynooth, Co. Kildare, Ireland
[b] Institute of Physiology II, University of Bonn, D-53115 Bonn, Germany
[c] National Institute for Cellular Biotechnology, Dublin City University, Dublin 9, Ireland

ARTICLE INFO

Keywords:
Biglycan
Dysferlin
Myelin PO
Myoferlin
Periaxin
Synemin

ABSTRACT

The highly progressive neuromuscular disorder dystrophinopathy is triggered by primary abnormalities in the *Dmd* gene, which causes cytoskeletal instability and loss of sarcolemmal integrity. Comparative organellar proteomics was employed to identify sarcolemma-associated proteins with an altered concentration in dystrophic muscle tissue from the *mdx-4cv* mouse model of dystrophinopathy. A lectin agglutination method was used to prepare a sarcolemma-enriched fraction and resulted in the identification of 190 significantly changed protein species. Proteomics established differential expression patterns for key components of the muscle plasma membrane, cytoskeletal network, extracellular matrix, metabolic pathways, cellular stress response, protein synthesis, immune response and neuromuscular junction. The deficiency in dystrophin and drastic reduction in dystrophin-associated proteins appears to trigger (i) enhanced membrane repair involving myoferlin, dysferlin and annexins, (ii) increased protein synthesis and the compensatory up-regulation of cytoskeletal proteins, (iii) the decrease in the scaffolding protein periaxin and myelin PO involved in myelination of motor neurons, (iv) complex changes in bioenergetic pathways, (v) elevated levels of molecular chaperones to prevent proteotoxic effects, (vi) increased collagen deposition causing reactive myofibrosis, (vii) disturbed ion homeostasis at the sarcolemma and associated membrane systems, and (viii) a robust inflammatory response by the innate immune system in response to chronic muscle damage.

Significance: Duchenne muscular dystrophy is a devastating muscle wasting disease and represents the most frequently inherited neuromuscular disorder in humans. Genetic abnormalities in the *Dmd* gene cause a loss of sarcolemmal integrity and highly progressive muscle fibre degeneration. Changes in the neuromuscular system are associated with necrosis, fibrosis and inflammation. In order to evaluate secondary changes in the sarcolemma membrane system due to the lack of the membrane cytoskeletal protein dystrophin, comparative organellar proteomics was used to study the *mdx-4cv* mouse model of dystrophinopathy. Mass spectrometric analyses identified a variety of altered components of the extracellular matrix-sarcolemma-cytoskeleton axis in dystrophic muscles. This included proteins involved in membrane repair, cytoskeletal restoration, calcium homeostasis, cellular signalling, stress response, neuromuscular transmission and reactive myofibrosis, as well as immune cell infiltration. These pathobiochemical alterations agree with the idea of highly complex secondary changes in X-linked muscular dystrophy and support the concept that micro-rupturing of the dystrophin-deficient plasma membrane is at the core of muscle wasting pathology.

1. Introduction

Skeletal muscle fibres endure high levels of load bearing and cellular shape change during lateral force transmission. The sarcolemma and its tight association with the basal lamina and associated extracellular matrix on the one hand, and bridging costameres and underlying intracellular cytoskeletal networks on the other hand, play a central role in the cytoarchitectural provision of mechanical stability for extended periods of excitation-contraction-relaxation cycles [1–3]. Mutations in genes that encode sarcolemma-associated or costamere-linked proteins, such as desmin, plectin, vinculin, talin, integrin or dystrophin and its associated glycoprotein complex, cause many types

* Corresponding author.
E-mail address: kay.ohlendieck@mu.ie (K. Ohlendieck).

https://doi.org/10.1016/j.jprot.2018.01.015
Received 16 October 2017; Received in revised form 12 January 2018; Accepted 28 January 2018
Available online 02 February 2018
1874-3919/

of muscular dystrophy [4]. Besides being of crucial importance for the protection of fibre integrity, the specialized and semi-permeable muscle plasmalemma and its invaginations also function as a physiological barrier with highly select cellular signalling, uptake and release mechanisms. This includes the provision of the subcellular structures, physiological systems and supramolecular complexes for efficient neurotransmission at the junctional folds, the propagation of action potentials towards the transverse tubular system, and excitation-contraction coupling from the neuromuscular junction towards the muscle interior [5].

The sarcolemma supports overall fibre shape and tissue elasticity in conjunction with the flexible components of the contractile apparatus and the attachment to the cytoskeleton. A key component involved in this process is the membrane cytoskeletal protein dystrophin [6], of which the full-length isoform Dp427-M [7] forms a scaffold for anchoring a variety of sarcolemmal proteins [8]. The dystrophin-glycoprotein complex provides the stabilising linkage between laminin-211 of the basal lamina and the cortical actin membrane cytoskeleton [9], besides being involved in signalling events at the muscle surface [10]. In the highly progressive muscle wasting disorder Duchenne muscular dystrophy, primary abnormalities in the *Dmd* gene cause the almost complete loss of full-length dystrophin and a concomitant reduction in dystrophin-associated proteins [11].

Mass spectrometry-based proteomics represents an ideal bioanalytical tool to investigate the complex secondary changes in dystrophin-deficient muscle tissues [12]. A variety of proteomic studies have analysed tissue extracts from various muscle types of animal models of X-linked muscular dystrophy [13–20]. Proteome-wide alterations were shown to occur in the contractile apparatus, metabolic pathways, signalling mechanisms, ion homeostasis, the cytoskeleton, the extracellular matrix and the cellular stress response [21–23]. In analogy, the study described here has extended and refined the proteomic survey of dystrophic skeletal muscles by focusing on the mass spectrometric identification of altered proteins in the sarcolemma-enriched fraction from the *mdx-4cv* animal model of dystrophinopathy. This particular genetic mouse model is lacking dystrophin due to a mutation in exon 53 [24] and the frequency of revertant fibres is considerably less as compared to the *mdx* mouse [25], which exhibits a mutation in exon 23 [26]. In this new and focused proteomic study, an agglutination affinity method was employed to isolate an enriched sarcolemmal preparation [27]. Sarcolemmal proteins present only a small percentage of the overall muscle protein constellation [28], which consists mostly of contractile and metabolic proteins [29]. This makes the proteomic evaluation of the sarcolemma membrane system technically challenging. However, since the primary pathobiochemical insult in dystrophinopathy is located in the sub-sarcolemmal cytoskeleton, it was of interest to study the closely associated sarcolemmal environment of the dystrophin network by organellar proteomics [30].

It is important to state that the interpretation of findings from subproteomic studies may be complicated due to both technical and pathobiochemical issues. On the one hand, subcellular fractionation procedures clearly reduce sample complexity and thus enable the analysis of low-abundance components, but on the other hand, the application of extensive isolation procedures for the enrichment of distinct membrane fractions may introduce potential bioanalytical artefacts. Complex pathophysiological processes, such as inflammation, necrosis or fibrosis [22], as well as cellular adaptations, may therefore distort the efficient isolation of distinct organelles and subsequent comparative proteomic profiling of mutant versus wild type membrane systems. However, independent verification experiments using immunoblotting or immunofluorescence microscopy can usually be used to confirm key findings from mass spectrometric surveys, and thus enable the objective evaluation of the validity of pathoproteomic profiles [12].

A select number of investigations that have utilized a combination of mass spectrometry, subcellular fractionation and interaction proteomics to study the dystrophin complex have confirmed the organization of the core complex consisting of dystrophin isoform Dp427-M, dystroglycans, sarcoglycans, sarcospan, syntrophins and dystrobrevins [27,31–33]. Additional linkages within the dystrophin complexome were shown to occur with nitric oxide synthase, biglycan, cytokeratin, synemin and the cytoskeletal linker desmoglein [34–38]. The findings from the proteomic survey described in this report have identified a variety of proteins of the basement membrane-sarcolemma-cytoskeleton axis with a significantly changed abundance in dystrophic muscles. This included sarcolemmal proteins, extracellular matrix components, cytoskeletal proteins and components of the motor neuron and associated glia cells. In addition, marker proteins of invading immune cells were detected at elevated levels indicating a considerable response by the innate immune system, which agrees with the occurrence of sterile inflammation in damaged muscle tissues.

2. Methods

2.1. Materials

For the comparative proteomic analysis of enriched sarcolemma preparations from wild type versus dystrophic *mdx-4cv* skeletal muscle, a variety of general analytical grade reagents and materials were obtained from GE Healthcare (Little Chalfont, Buckinghamshire, UK), Bio-Rad Laboratories (Hemel-Hempstead, Hertfordshire, UK) and Sigma Chemical Company (Dorset, UK). Ultrapure acrylamide stock solutions were purchased from National Diagnostics (Atlanta, GA, USA), sequencing grade modified trypsin and Lys-C were obtained from Promega (Madison, WI, USA) and Whatman nitrocellulose transfer membranes came from Invitrogen (Carlsbad, CA, USA). The chemiluminescence substrate and protease inhibitors were purchased from Roche Diagnostics (Mannheim, Germany). Primary antibodies for immunoblotting and immunofluorescence microscopy were purchased from Abcam, Cambridge, UK (ab43125 to β-dystroglycan, ab124798 to desmoglein isoform DSG1, ab2413 to fibronectin, ab58562 to biglycan, and ab124684 to dysferlin), LifeSpan Biosciences, Seattle, WA, USA (LS-B11314 to myoferlin), Sigma Chemical Company, Dorset, UK (L9393 to laminin), EMD Millipore, Schwalbach am Taunus, Germany (ABN363 to myelin PO protein), BD Transduction Laboratories, Heidelberg, Germany (A14020 to annexin A2), and NovoCastra, Leica Biosystems, Newcastle Upon Tyne, UK (NCL-Dys2 to the carboxy terminus of dystrophin isoform Dp427). Chemicon International (Temecula, CA, USA) provided peroxidase-conjugated secondary antibodies. For immunofluorescence microscopy, normal goat serum and goat-anti-mouse IgG RRX (Rhodamine Red-X) antibodies were purchased from Molecular Probes, Life Technologies (Darmstadt, Germany). The embedding medium Fluoromount G was from Southern Biotech (Birmingham, AL, USA). Purified wheat germ lectin, *N*-acetyl-D-glucosamine and bis-benzimide Hoechst-33342 were obtained from Sigma Chemical Company (Dorset, UK).

2.2. Dystrophic mdx-4cv mouse model of Duchenne muscular dystrophy

First described in 1989 [39], the *mdx-4cv* mouse model was generated on the C57BL/6 background by chemical mutagenesis using *N*-ethyl-nitrosourea. The induced C to T transition at base 7916 in exon 53 of the dystrophin gene generates a premature stop codon, thus abrogating dystrophin synthesis. The *mdx-4cv* mouse exhibits a number of histopathological features of dystrophinopathy and has the added advantage of possessing 10-fold fewer dystrophin-positive revertant fibres than the conventionally used *mdx* mouse model [25]. For the identification of global changes in the sarcolemmal proteome, total tissue extracts of hind limb muscle from 5-month-old control C57BL/6 mice and age-matched *mdx-4cv* mice were obtained from the Bioresource Unit of the University of Bonn. Mice were kept under standard conditions and all procedures adhered to German and Irish legislation on the use of

animals in experimental research. The animals were sacrificed by cervical dislocation and hind limbs were carefully dissected and quick-frozen in liquid nitrogen [16]. Samples were transported to Maynooth University in accordance with the Department of Agriculture (animal by-product register number 2016/16 to the Department of Biology, National University of Ireland, Maynooth) and stored at −80 °C prior to analysis.

2.3. Preparation of crude muscle microsomes from normal and dystrophic hind leg muscle

Hind limb muscle specimens were from age-matched normal versus dystrophic animals (4 g wet weight; $n = 3$). For each biological replicate three hind legs from three different mice were pooled. In total nine hind legs were used to generate three biological replicates each for wild-type and *mdx-4cv* specimens. The samples were finely chopped and homogenised in 7.5 volumes of homogenisation buffer (20 mM sodium pyrophosphate, 20 mM sodium phosphate, 1 mM $MgCl_2$, 0.303 M sucrose, 0.5 mM EDTA, pH 7.0, supplemented with a protease inhibitor cocktail [20]), using a hand-held IKA T10 Basic Homogeniser from IKA Labortechnik (Staufen, Germany). Crude muscle homogenates were kept on ice for 1.5 h and subsequently centrifuged at 14,000*g* for 15 min at 4 °C. The protein containing supernatant was removed and centrifuged at 100,000*g* for 1 h at 4 °C [40] using an Optima L-100 XP ultracentrifuge from Beckman Coulter (Fullerton, CA, USA). The resulting pellet containing crude microsomes was re-suspended in an appropriate volume of 50 mM sodium phosphate, 0.16 M NaCl, pH 7.4.

2.4. Preparation of enriched sarcolemma by wheat germ agglutination

An enriched sarcolemma preparation was prepared from crude microsomes using age-matched wild type versus dystrophic *mdx-4cv* mice with the help of an established lectin agglutination method, as previously described in detail [27,28,41]. Briefly, crude microsomes were diluted with 50 mM sodium phosphate, 0.16 M NaCl, pH 7.4 to give a final protein concentration of 1 mg/ml. This suspension was added to an equal volume of 1 mg/ml wheat germ lectin in above buffer, mixed gently and kept on ice for 10 min. This mixture was pelleted at 14,000*g* for 90 s. The supernatant from this centrifugation step contained non-agglutinated vesicles. The pellet was re-suspended in 20 mM Tris-HCl, pH 7.4, 0.303 M sucrose, and centrifuged again at 14,000*g* for 90 s. This step was repeated once more. The resulting pellets were re-suspended in the above described Tris buffer and de-agglutinated by incubation with the competitive sugar 0.2 M *N*-acetyl-D-glucosamine for 20 min at room temperature [28]. The de-agglutinated suspension was centrifuged at 14,000*g* for 90 s, and the resulting supernatant was pelleted at 150,000*g* for 20 min at 4 °C in an Optima L-100 XP ultracentrifuge (Beckman Coulter, Fullerton, CA, USA). The pellet from this step was re-suspended in above buffer and centrifuged again at 150,000*g* for 20 min at 4 °C. This pellet corresponds to a subcellular fraction enriched in sarcolemma vesicles [41]. Membranes were re-suspended in an appropriate volume of label-free solubilisation buffer (6 M urea, 2 M thiourea, 10 mM Tris, pH 8.0 in LC-MS grade water) for subsequent label-free mass spectrometry.

2.5. Sample preparation for label-free liquid chromatography mass spectrometry

Protein concentrations of enriched sarcolemma samples were determined using the Bradford assay system [42] and sample volumes were then equalised with label-free solubilisation buffer. Samples for LC-MS/MS analysis were reduced with 10 mM dithiothreitol for 30 min at room temperature, and alkylated with 25 mM iodoacteamide in 50 mM ammonium bicarbonate for 20 min at room temperature in the dark. A further 10 mM dithiothreitol was added to each sample and then incubated for 15 min at room temperature in the dark, to quench any unreacted iodoacteamide [18]. Proteolytic digestion was achieved using a combination of the enzymes Lys-C and trypsin. Samples were first digested with sequencing grade Lys-C at a ratio of 1:100 (protease:protein) and incubated at 37 °C for 4 h. Samples were then diluted with four times the initial sample volume with 50 mM ammonium bicarbonate, followed by digestion with sequencing grade modified trypsin at a ratio of 1:25 (protease:protein) overnight at 37 °C [43]. The addition of 2% trifluoroacetic acid (TFA) in 20% acetonitrile (ACN) (3:1 (v/v) dilution) was used to stop proteolytic digestion. The peptides were purified using Pierce C18 spin columns from Thermo Fisher Scientific (Dublin, Ireland), dried through vacuum centrifugation and re-suspended in an appropriate volume of loading buffer (2% ACN, 0.05% TFA in LC-MS grade water). Peptide suspensions were vortexed and sonicated to aid full re-suspension. Samples were centrifuged briefly at 14,000*g* and the supernatant transferred to mass spectrometry vials.

2.6. Label-free liquid chromatography mass spectrometry

The label-free liquid chromatography mass spectrometric (LC-MS/MS) analysis of enriched sarcolemma from wild type versus *mdx-4cv* tissue was carried out using an Ultimate 3000 NanoLC system (Dionex Corporation, Sunnyvale, CA, USA) coupled to a Q-Exactive mass spectrometer (Thermo Fisher Scientific). Peptide mixtures (4 µl, corresponding to 0.8 µg protein) were loaded by an autosampler onto a C18 trap column (C18 PepMap, 300 µm id × 5 mm, 5 µm particle size, 100 Å pore size; Thermo Fisher Scientific). The trap column was switched online with an analytical Biobasic C18 Picofrit column (C18 PepMap, 75 µm id × 50 cm, 2 µm particle size, 100 Å pore size; Dionex) [44]. Peptides were eluted from the column using the following binary gradient: solvent A [2% (v/v) ACN and 0.1% (v/v) formic acid in LC-MS grade water] and 0–90% solvent B [80% (v/v) ACN and 0.1% (v/v) formic acid in LC-MS grade water]. The peptides were eluted as follows: 5–45% solvent B for the first 120 min, 45–90% solvent B for 2.5 min, 90% solvent B for 7 min and 3% solvent B for 43 min. The column flow rate was set to 0.3 µl/min [45]. Data were acquired with Xcalibur software (Thermo Fisher Scientific). The Q-Exactive was operated in positive, data-dependent mode and was externally calibrated. Survey MS scans were performed in the 300–1700 m/z range with a resolution of 140,000 (m/z 200) and lock mass set to 445.12003. CID (collision-induced dissociation) fragmentation was carried out with the fifteen most intense ions per scan and at 17,500 resolution. A dynamic exclusion window was applied within 30 s. An isolation window of 2 m/z and one microscan were used to collect suitable tandem mass spectra. Pre-run and post-run HeLa protein samples were analysed by Proteome Discoverer 1.4 to verify the reproducibility of the LC-MS/MS system.

2.7. Protein profiling by label-free LC-MS/MS

To determine the degree of enrichment of sarcolemmal proteins and potential dystrophin-associated proteins, mass spectrometric files were first searched qualitatively against the UniProtKB-SwissProt *Mus musculus* database using Proteome Discoverer 1.4 (Thermo Fisher) and Sequest HT (SEQUEST HT algorithm, licence Thermo Scientific, registered trademark University of Washington, USA). The following settings were used: (i) peptide mass tolerance set to 10 ppm, (ii) MS/MS mass tolerance set to 0.02 Da, (iii) a maximum of two missed cleavages, (iv) carbamidomethylation set as a fixed modification (v) methionine oxidation set as a variable modification and (vi) peptide confidence set to high. Subsequently Progenesis QI for Proteomics software (version 3.1; Non-Linear Dynamics, a Waters company, Newcastle upon Tyne, UK) was used for the quantitative analysis of enriched sarcolemma from wild-type versus *mdx-4cv* skeletal muscle. A reference run was selected and all other runs were aligned to this run, thus allowing for any drift in retention time [46]. Prior to being exported as a MASCOT generic file (mgf) to Proteome Discoverer 2.1 (Thermo Scientific) the MS/MS data files were filtered using the following settings: (i) peptide features with

ANOVA ≤ 0.01 between experimental groups, (ii) mass peaks with charge states from +1 to +5 and (iii) greater than one isotope per peptide. Protein identification was performed using Proteome Discoverer 2.1 against Mascot (version 2.3, Matrix Science, Boston, MA, USA) and Sequest HT using the UniProtKB-SwissProt *Mus musculus* database. The following search parameters were used: (i) peptide mass tolerance set to 10 ppm, (ii) MS/MS mass tolerance set to 0.02 Da, (iii) up to two missed cleavages, (iv) carbamidomethylation set as a fixed modification and (v) methionine oxidation set as a variable modification [47]. For re-importation back into Progenesis LC-MS software as a PepXML file only peptides with either ion scores of 40.00 or more (from Mascot) and peptides with XCorr scores ≥ 1.5 (from Sequest HT) were allowed. The following criteria were applied to assign proteins as positively identified: (i) an ANOVA score between experimental groups of ≤0.01, and (ii) proteins with ≥2 peptides matched.

The freely available software packages PANTHER (http://pantherdb.org/), STRING (https://string-db.org/) and the web-based gene set analysis toolkit named WebGestalt (http://www.webgestalt.org/webgestalt_2013/) were used to identify protein class, characterize potential protein interactions and classify the cellular location of identified proteins respectively.

2.8. Comparative immunoblot analysis

For the independent evaluation of potential protein changes identified by mass spectrometry, a comparative immunoblot survey with a panel of specific antibodies to select muscle proteins was carried out using total crude extracts from 5-month-old wild-type and age-matched *mdx-4cv* hind limb muscle tissue. One-dimensional gel electrophoresis, silver staining of protein gels and immunoblot analysis was performed as previously described in detail [47]. Briefly, samples for immunoblot analysis were prepared in 2× Laemmli buffer heated at 97 °C for 7 min and loaded onto hand-cast 10% sodium dodecyl sulfate polyacrylamide gels. For comparative analyses, silver staining of protein gels was carried out with 10 μg protein per lane. Immunoblotting was carried out with 25 μg of protein per lane, with the exception of myelin protein, which was analysed with 50 μg of protein per gel lane. Proteins were transferred to nitrocellulose membranes, blocked and incubated in primary antibody overnight, followed by detection with horseradish peroxidase conjugated secondary antibodies using the enhanced chemiluminescence method. Densitometric scanning and statistical analysis of immunoblots was performed using a HP PSC-2355 scanner and ImageJ software (NIH, Bethesda, MD, USA) along with Graph-Pad Prism software (San Diego, CA, USA), in which statistical significance was based on a p value ≤ 0.05.

2.9. Immunofluorescence microscopy

The immunofluorescence microscopical localization of dystrophin and myoferlin was carried out with wild type versus *mdx-4cv* skeletal muscles. Freshly dissected tissue specimens were quick-frozen in liquid nitrogen-cooled isopentane and 10 μm sections cut in a cryostat [20]. For dystrophin immuno-staining, unfixed cryosections were boiled in phosphate-buffered saline for 5 min as previously described in detail [48]. Tissue sections were permeabilised in 0.1% (v/v) Triton X-100 for 10 min and then blocked with 1:20 diluted normal goat serum for 30 min at room temperature. For myoferlin immuno-staining, muscle tissue sections were fixed in acetone for 10 min at room temperature and then also blocked with normal goat serum as described above. Primary antibodies to dystrophin and myoferlin were diluted 1:20 and 1:50, respectively, in phosphate-buffered saline for overnight incubation at 4 °C [20]. Specimens were carefully washed and then incubated with fluorescently-labelled secondary antibodies, using 1:200 diluted anti-mouse RRX antibody for 45 min at room temperature. Nuclei were counter-stained with 1 μg/ml bis-benzimide Hoechst 33342. Following antibody labelling, tissue sections were embedded in Fluoromount G medium and viewed under a Zeiss Axioskop 2 epifluorescence microscope equipped with a digital Zeiss AxioCam HRc camera (Carl Zeiss Jena GmbH, Jena, Germany).

3. Results

3.1. Proteomic analysis of the sarcolemma-enriched fraction from skeletal muscle

The isolation of sufficient quantities of the sarcolemma-enriched fraction from mouse skeletal muscle for extensive biochemical analyses is difficult and results in relatively small amounts of membrane vesicles. Using differential centrifugation in combination with lectin agglutination, the affinity purification method employed in this study yielded approximately 70 μg protein per 4 g of starting material. However, these low amounts of membranes were sufficient to carry out a comparative proteomic study on wild type versus *mdx-4cv* skeletal muscle tissue. The sarcolemma-enriched fraction contains the plasma membrane region and its actin membrane cytoskeleton and associated intracellular cytoskeleton, and the basal lamina and extracellular matrix, as well as the neuromuscular junction and attached motor neuron and Schwann cells [27,28,41]. In addition, abundant membranes and protein populations from mitochondria, the sarcoplasmic reticulum, transverse tubules, ribosomes, the Golgi apparatus, the nucleus, the cytosol, lysosomes, serum and the contractile apparatus are usually present in agglutinated vesicle preparations from skeletal muscle tissue [27]. The previous biochemical evaluation of the Dp427 isoform of dystrophin in *mdx* sarcolemma preparations using gradient gel electrophoresis and immunoblotting [49] suggests a similar degree of cross-contaminations in mouse membranes as compared to rabbit preparations [27]. The gel electrophoretic protein band pattern of the wild type versus the dystrophin-deficient mouse sarcolemma fraction was shown to be relatively comparable. However, besides sarcolemma vesicles, a major class of membranes is derived from the sarcoplasmic reticulum, as illustrated by the presence of a major band of apparent 110 kDa consisting of SR Ca^{2+}-ATPases and a high-molecular-mass band above dystrophin of apparent 560 kDa that represents the RyR1 isoform of the ryanodine receptor calcium-release channel [49]. Fig. 1 illustrates the distribution of cellular components in the isolated membrane fraction from wild type and *mdx-4cv* preparations, including membranes, mitochondria, macromolecular complexes, envelope, nucleus, endoplasmic reticulum, membrane-enclosed lumen, cytoskeleton, cell projection and the endomembrane system.

The multi-consensus files of identified protein species with high confidence qualitative results confirmed the presence of crucial members of the sarcolemmal dystrophin-glycoprotein complex and key sarcolemmal marker proteins. The core dystrophin complex was represented by dystrophin isoform Dp427 (P11531), α/β-dystroglycan (Q62165), α-sarcoglycan (P82350), β-sarcoglycan (P82349), γ-sarcoglycan (P82348), δ-sarcoglycan (P82347), α1-syntrophin (Q61234) and sarcospan (Q62147). Sarcolemmal marker proteins included dysferlin (Q9ESD7), the plasma membrane Ca^{2+}-transporting ATPase isoform Atp2b1 (G5E829), various subunits of the Na^+/K^+-ATPase (Q8VDN2, Q6PIE5, P14094, P97370, P14231), integrins (P05555, P09055, O70309, Q3V3R4, P43406), annexins A1 and A2 (P10107, P07356), Na^+-channel subunits (Q9ER60, P97952, Q7M729) and the sarcolemmal Cl^--channel protein (Q64347). Motor neuron and myelinating Schwann cell-derived markers were identified as the neural cell adhesion molecule NCAM-1 (P13595-4), the synaptosomal-associated protein SNAP-23 (O09044), neuroplastin (P97300-3), dystrophin-related protein DRP-2 (Q05AA6), periaxin (O55103), myelin basic protein (P04370-4), myelin protein PO (P27573) and myelin protein P2 (P24526).

Components of the sarcolemma-attached basal lamina and extracellular matrix were identified as laminin (Q60675, P02468, P02469), nidogen (P10493), basement membrane-specific heparan sulfate

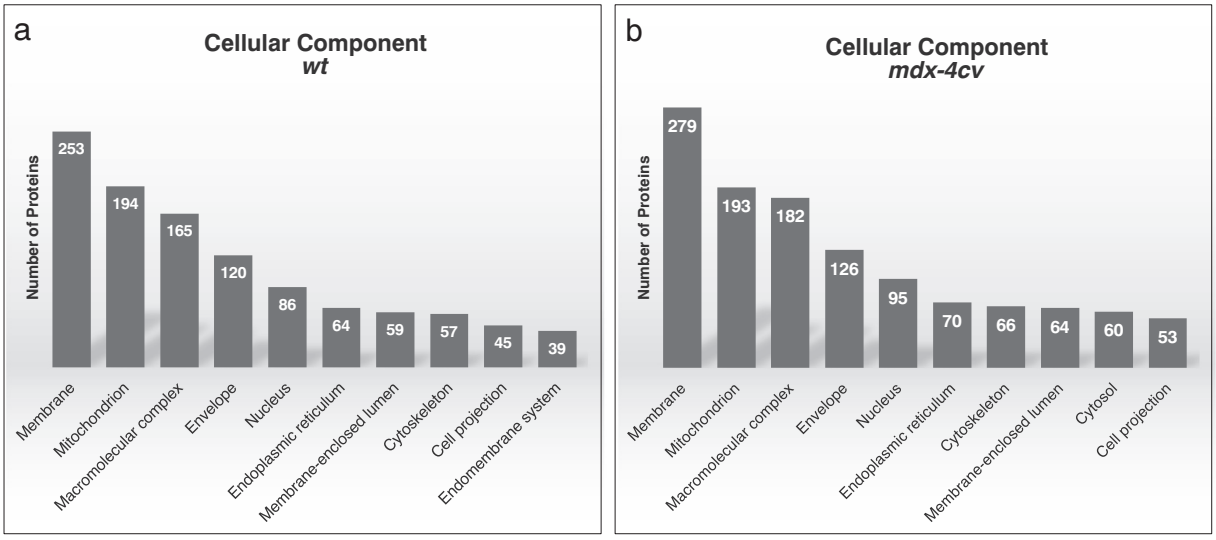

Fig. 1. Overview of the subcellular localization of proteins identified in the sarcolemma-enriched fraction from wild type (a, *wt*) and dystrophic (b, *mdx-4cv*) mice by mass spectrometry-based proteomics using multi-consensus data. Shown are the top 10 cellular components based on WebGestalt analysis, filtered on high confidence peptides and on Xcorr scores (default on Proteome Discover), and only for proteins ≥2 unique peptides.

proteoglycan core protein HSPG-2 (Q05793), collagen VI (Q02788, Q04857), decorin (P28654), lumican (P51885), prolargin (Q9JK53) and asporin (Q99MQ4). Cytoskeletal proteins associated with the muscle plasma membrane included synemin (Q70IV5-2), vimentin (P20152), desmin (P31001), tubulin (P99024, P68369) and vinculin (Q64727).

3.2. Decreased proteins in dystrophin-deficient sarcolemma from mdx-4cv muscle

The comparative proteomic analysis of the sarcolemma-enriched fraction revealed that the full-length Dp427 isoform of dystrophin (accession number P11531; gene name *Dmd*), which was recognized by 8 unique peptides (Table 1), is the most reduced protein species in *mdx-4cv* hind limb muscle. This agrees with the mutant status of the *mdx-4cv* mouse model of Duchenne muscular dystrophy. In analogy, the main dystrophin-associated glycoproteins α/β-dystroglycan, α-sarcoglycan and δ-sarcoglycan were shown be greatly reduced in the sarcolemma fraction from dystrophic skeletal muscles (Table 1). In addition, the dystrophin-associated glycoprotein β-sarcoglycan (accession number P82349; gene name *Sgcb*) was recognized by 1 unique peptide (confidence 41.49; Anova (p) 7.17E-05) and showed a 7.6-fold decrease. Besides the dystrophin complex, the expression levels of a variety of metabolic enzymes, components of the motor neuron system,

Table 1
Mass spectrometric identification of proteins with a reduced abundance in the sarcolemma-enriched fraction from dystrophic *mdx-4cv* skeletal muscle.

Accession	Gene name	Protein name	Unique peptides	Peptide count	Confidence score	Anova (p)	Max fold change
P11531	Dmd	Dystrophin	8	8	255.9	1.26E-05	2708.2
P27573	Mpz	Myelin protein P0	2	2	4.6	2.84E-05	33.8
O55103	Prx	Periaxin	15	15	566.6	1.95E-11	21.8
Q8BKZ9	Pdhx	Pyruvate dehydrogenase protein X component, mitochondrial	2	2	98.2	1.76E-05	16.8
Q62165	Dag1	Dystroglycan	2	2	51.6	1.03E-07	14.8
P41216	Acsl1	Long-chain-fatty-acid–CoA ligase 1	3	3	174.0	9.99E-04	12.2
Q99LC3	Ndufa10	NADH dehydrogenase [ubiquinone] 1 alpha subcomplex subunit 10, mitochondrial	2	2	62.5	1.97E-04	8.2
Q8VCT4	Ces1d	Carboxylesterase 1D	2	2	82.2	1.64E-04	6.8
Q70IV5	Synm	Synemin	2	2	47.7	4.99E-06	5.3
P16330	Cnp	2′,3′-cyclic-nucleotide 3′-phosphodiesterase	3	3	85.5	2.10E-04	4.9
P12367	Prkar2a	cAMP-dependent protein kinase type II-alpha regulatory subunit	2	2	3.2	6.95E-05	4.9
A2A863	Itgb4	Integrin beta-4	5	5	160.7	8.49E-05	4.3
P82347	Sgcd	Delta-sarcoglycan	3	3	57.6	3.78E-04	4.0
P82350	Sgca	Alpha-sarcoglycan	2	2	118.5	3.63E-06	3.7
Q8R1G2	Cmbl	Carboxymethylenebutenolidase homolog	2	2	43.1	3.15E-03	3.5
P09411	Pgk1	Phosphoglycerate kinase 1	2	2	3.2	2.01E-06	3.3
P05064	Aldoa	Fructose-bisphosphate aldolase A	2	2	49.3	3.86E-05	3.3
Q64521	Gpd2	Glycerol-3-phosphate dehydrogenase, mitochondrial	2	2	83.6	2.75E-04	3.2
Q8BH59	Slc25a12	Calcium-binding mitochondrial carrier protein Aralar1	3	3	129.9	1.55E-03	3.2
Q8R3Z5	Cacnb1	Voltage-dependent L-type calcium channel subunit beta-1	2	2	95.2	1.25E-05	3.1
O09165	Casq1	Calsequestrin-1	2	2	50.3	3.30E-04	3.0
P07310	Ckm	Creatine kinase M-type	2	2	72.7	6.54E-03	2.9
Q03265	Atp5a1	ATP synthase subunit alpha, mitochondrial	3	3	107.2	2.52E-05	2.6
P61982	Ywhag	14–3-3 protein gamma	2	2	57.3	5.13E-06	2.4
Q61554	Fbn1	Fibrillin-1	4	4	183.3	2.41E-03	2.2
Q7TQ48	Srl	Sarcalumenin	3	3	5.6	4.52E-03	1.7
P14824	Anxa6	Annexin A6	3	3	216.8	1.17E-03	1.6

Table 2
Mass spectrometric identification of proteins with an increased abundance in the sarcolemma-enriched fraction from dystrophic *mdx-4cv* skeletal muscle. Additional proteins with an increased abundance change below 5-fold are listed in Table 1 in the accompanying Data-in-Brief publication [50].

Accession	Gene name	Protein name	Unique peptides	Peptide count	Confidence score	Anova (p)	Max fold change
P49290	Epx	Eosinophil peroxidase	2	2	3.6	1.60E-13	Infinity
P04441	Cd74	H-2 class II histocompatibility antigen gamma chain	2	2	3.2	1.32E-04	117.4
Q9D1I2	Card19	Caspase recruitment domain-containing protein 19	2	2	57.0	7.26E-04	60.7
Q5SX39	Myh4	Myosin-4	5	5	115.6	5.01E-03	32.9
Q9D0E1	Hnrnpm	Heterogeneous nuclear ribonucleoprotein M	2	2	45.8	5.08E-03	32.3
Q5SX40	Myh1	Myosin-1	15	15	800.4	8.51E-04	27.1
P13541	Myh3	Myosin-3	2	2	3.7	4.28E-03	22.7
P01901	H2-K1	H-2 class I histocompatibility antigen, K-B alpha chain	4	4	202.7	1.68E-07	20.1
P06800	Ptprc	Receptor-type tyrosine-protein phosphatase C	3	3	214.0	2.87E-07	20.0
P97457	Mylpf	Myosin regulatory light chain 2, skeletal muscle isoform	2	2	143.6	9.78E-04	17.2
P62918	Rpl8	60S ribosomal protein L8	3	3	105.0	1.05E-06	13.3
P47964	Rpl36	60S ribosomal protein L36	2	2	3.3	9.55E-03	13.0
Q8BMD8	Slc25a24	Calcium-binding mitochondrial carrier protein SCaMC-1	4	4	214.4	2.91E-05	12.7
Q62230	Siglec1	Sialoadhesin	6	6	302.8	6.83E-05	10.8
P62301	Rps13	40S ribosomal protein S13	2	2	62.7	2.35E-05	10.6
P51881	Slc25a5	ADP/ATP translocase 2	2	2	97.3	1.98E-05	10.3
Q8BMK4	Ckap4	Cytoskeleton-associated protein 4	7	7	229.0	2.47E-05	10.3
Q9D8E6	Rpl4	60S ribosomal protein L4	4	4	97.0	1.01E-05	9.9
P47911	Rpl6	60S ribosomal protein L6	3	3	162.4	4.38E-07	9.4
P43276	Hist1h1b	Histone H1.5	4	4	62.0	1.14E-05	8.9
P62245	Rps15a	40S ribosomal protein S15a	3	3	158.8	4.86E-06	8.5
P11835	Itgb2	Integrin beta-2	3	3	102.8	1.04E-04	8.0
Q69ZN7	Myof	Myoferlin	5	5	121.4	1.62E-04	7.8
P01872	Ighm	Ig mu chain C region	3	3	149.1	4.53E-05	7.4
Q7TPR4	Actn1	Alpha-actinin-1	2	2	42.5	2.98E-05	6.7
Q6ZWV7	Rpl35	60S ribosomal protein L35	2	2	47.0	2.17E-05	6.7
P14148	Rpl7	60S ribosomal protein L7	3	3	109.4	5.97E-08	6.6
Q9D8H7	Oma1	Metalloendopeptidase OMA1, mitochondrial	2	2	4.0	8.43E-07	6.6
P49300	Clec10a	C-type lectin domain family 10 member A	3	3	102.0	6.37E-05	6.5
P47963	Rpl13	60S ribosomal protein L13	2	2	47.6	3.83E-08	6.4
Q9WV54	Asah1	Acid ceramidase	3	3	105.4	1.62E-07	6.4
P28653	Bgn	Biglycan	2	2	116.0	3.31E-04	6.4
P62754	Rps6	40S ribosomal protein S6	2	2	43.9	5.97E-07	6.4
P43274	Hist1h1e	Histone H1.4	6	6	68.9	1.83E-06	6.3
P35979	Rpl12	60S ribosomal protein L12	2	2	64.4	3.07E-04	6.1
Q9CR57	Rpl14	60S ribosomal protein L14	3	3	190.3	1.22E-05	6.1
Q3UMR5	Mcu	Calcium uniporter protein, mitochondrial	3	3	130.5	1.43E-05	5.7
Q62465	Vat1	Synaptic vesicle membrane protein VAT-1 homolog	3	3	195.2	2.85E-05	5.7
P53026	Rpl10a	60S ribosomal protein L10a	2	2	55.8	2.67E-05	5.5
P97449	Anpep	Aminopeptidase N	4	4	119.0	3.53E-05	5.5
O88990	Actn3	Alpha-actinin-3	8	8	449.6	2.18E-04	5.5
P50285	Fmo1	Dimethylaniline monooxygenase [N-oxide-forming] 1	2	2	67.5	3.49E-04	5.4
P54116	Stom	Erythrocyte band 7 integral membrane protein	5	5	308.7	8.74E-05	5.3
Q923B6	Steap4	Metalloreductase STEAP4	3	3	79.0	1.16E-04	5.3
P29788	Vtn	Vitronectin	2	2	93.6	6.84E-09	5.3
Q64449	Mrc2	C-type mannose receptor 2	3	3	112.7	2.78E-06	5.3
P10107	Anxa1	Annexin A1	3	3	191.0	1.28E-05	5.2
Q8VHX6	Flnc	Filamin-C	4	4	62.2	3.76E-05	5.1
P62702	Rps4x	40S ribosomal protein S4, X isoform	4	4	68.2	9.56E-06	5.0

cytoskeletal proteins, sarcolemmal receptors and ion-handling proteins were shown to be reduced. Proteins with decreased abundance in the sarcolemma-enriched fraction, which were only identified by a single unique peptide, are listed in the accompanying Data-in-Brief publication [50].

3.3. Increased proteins in dystrophin-deficient sarcolemma from mdx-4cv muscle

A large number of proteins with an increased abundance in the sarcolemma-enriched fraction from *mdx-4cv* muscle tissue were identified by mass spectrometric analysis. As listed in Table 2**,** and Table 1 in the accompanying Data-in-Brief publication [50], protein species with a significant change ranged from eosinophil-derived granule peroxidase to NADPH-dependent retinol dehydrogenase. The proteomic survey revealed drastic increases in proteins that function in the response of the innate immune system, inflammation, various aspects of cytosolic and mitochondrial metabolism, fibre regeneration, the contractile apparatus, ribosomal protein synthesis, Ca^{2+}-regulation, maintenance of membrane potential, cell adhesion processes, the cellular stress response, the cytoskeletal network and the extracellular matrix. Changes in isoforms of contractile proteins and Ca^{2+}-handling proteins indicate alterations in the fine regulation of the actomyosin apparatus and the kinetics of ion fluxes involved in excitation-contraction coupling in muscular dystrophy. In relation to the dystrophic phenotype and sarcolemmal adaptations, an interesting finding was the 7.8-fold increase in the plasma membrane repair protein myoferlin (Table 2). Importantly, this member of the ferlin protein family is highly homologous to the plasmalemmal protein dysferlin, which was also identified in this study, but only by 1 peptide (accession number Q9ESD7; gene name *Dysf*; confidence 47.53; Anova (p) 0.002839315). Dysferlin was shown to exhibit a 2.8-fold increase in abundance in the fraction with *mdx-4cv* muscle sarcolemma. In addition, proteins with increased abundance in the sarcolemma-enriched fraction, which were only identified by a single unique peptide, are listed in the accompanying Data-in-Brief publication [50].

The distribution of proteomic changes is summarized in the bioinformatic PANTHER diagramme of Fig. 2, which illustrates the wide

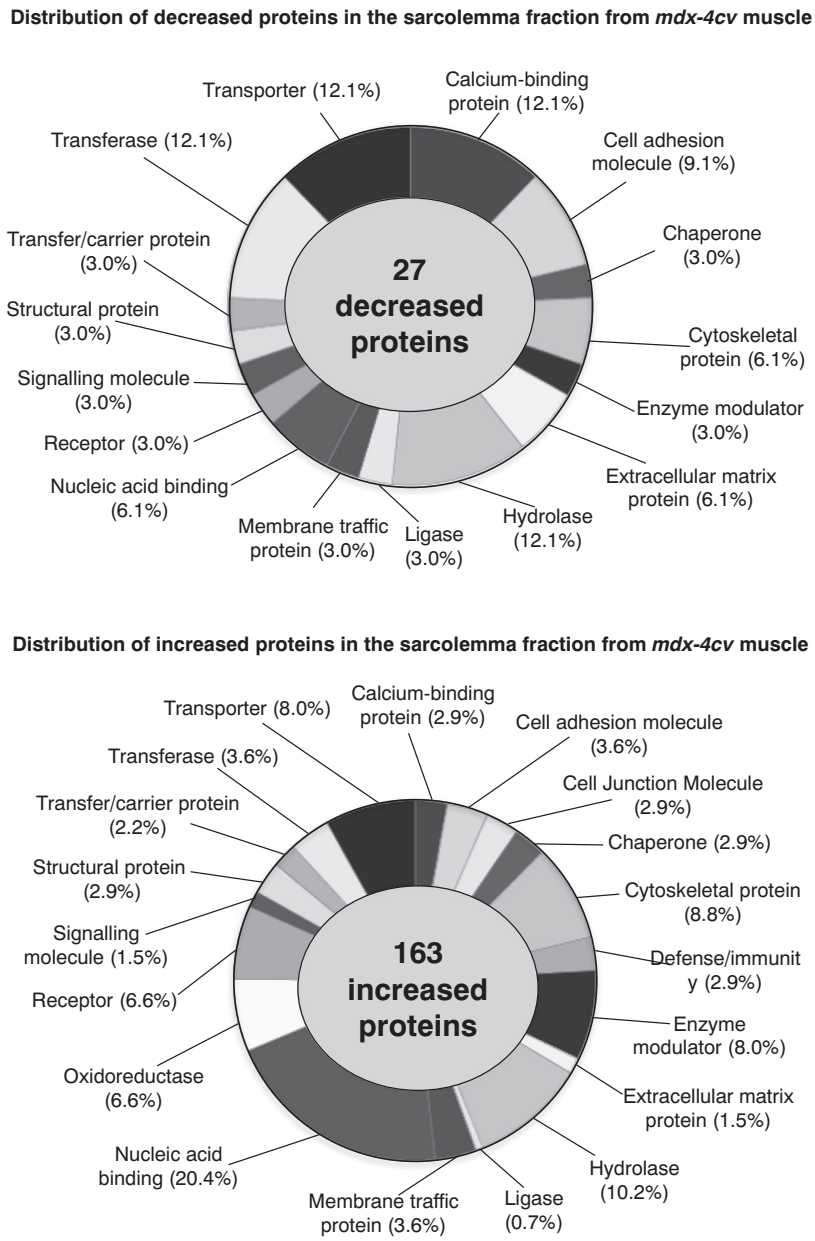

Fig. 2. Overview of changed protein classes in the sarcolemma-enriched fraction from *mdx-4cv* skeletal muscle. In order to identify the clustering of decreased (a) and increased (b) protein classes based on the mass spectrometric analysis of sarcolemma preparations from wild type versus *mdx-4cv* skeletal muscles (Tables 1, 2 and S1), the bioinformatics software programme PANTHER was used.

range of altered biological functions in muscular dystrophy. The listings of changed proteins includes 27 decreased proteins (Fig. 2a) and 163 increased proteins (Fig. 2b). Potential protein-protein interaction patterns within the altered protein population in the sarcolemma-enriched fraction from *mdx-4cv* skeletal muscles were determined with the STRING analysis programme. Fig. 3 shows the network analysis of decreased versus increased protein species. Interesting patterns emerged from the decreased core dystrophin complex, consisting of dystrophin isoform Dp427, dystroglycan and sarcoglycans, and its interactions via dystroglycan with the Schwann cell scaffolding protein periaxin and myelin protein PO, as well as the Ca^{2+}-regulatory system (Fig. 3a). Two major clusters were identified in the increased protein constellation, i.e. the 40S ribosomal proteins SA, S2, S3, S4, S6, S8, S9, S11, S13, S15, S16, S18, S23, S25 and the 60S ribosomal proteins L4, L6, L7, L8, L12, L13, L14, L18, L35, L36 forming supramolecular networks, and the cytoskeleton-contractile apparatus-extracellular matrix axis (Fig. 3b). The bioinformatic analysis of the proteomic data sets generated in this survey of the dystrophin-deficient sarcolemma suggests complex pathophysiological changes in a variety of cellular systems and potential compensatory mechanisms involving protein synthesis, changes in contractile protein isoforms and the up-regulation of cytoskeletal proteins.

3.4. Verification of proteomic changes by immunoblot analysis

Key findings from the proteomic analysis of the sarcolemma-enriched fraction from *mdx-4cv* skeletal muscles were verified by immunoblotting. However, a serious issue with many commercially available antibodies is a lack of species, tissue and/or protein isoform specificity to achieve a satisfactory signal-to-noise ratio. A large number of tested antibodies to newly identified proteins resulted in extensive background staining, which prevented their proper assessment by immunoblot analysis (not shown). Fig. 4 shows the successful immunoblotting of 8 different proteins, including newly identified

a **Potential protein-protein interaction pattern of decreased proteins in the sarcolemma fraction from *mdx-4cv* muscle**

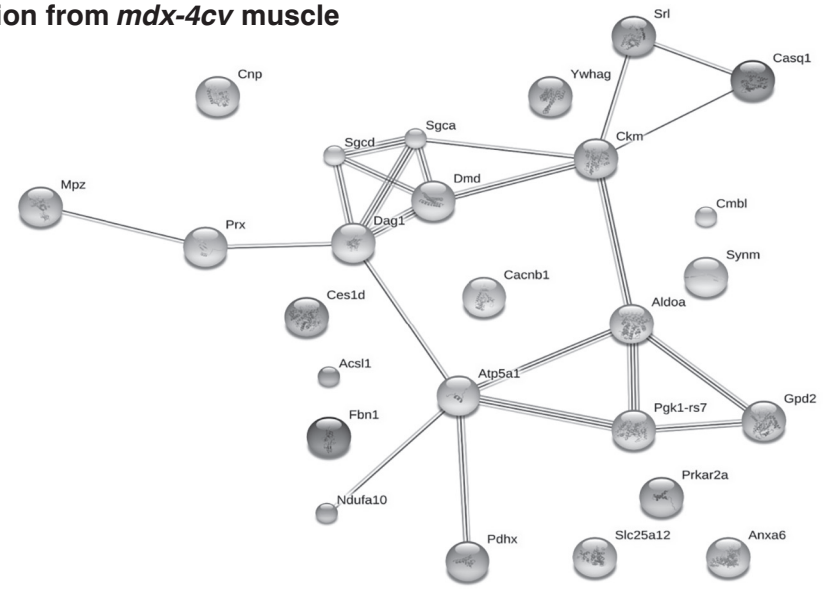

b **Potential protein-protein interaction pattern of increased proteins in the sarcolemma fraction from *mdx-4cv* muscle**

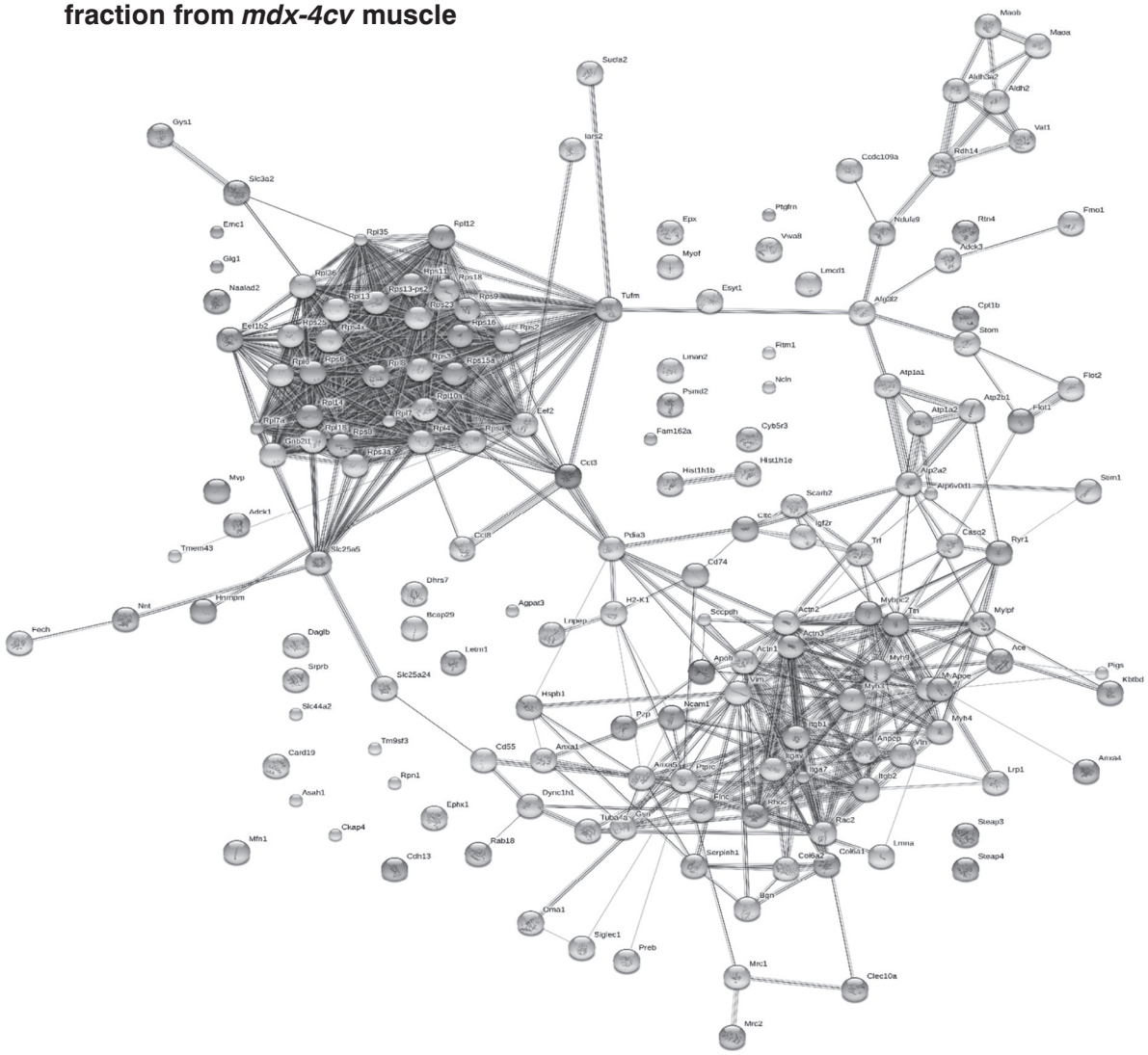

Fig. 3. Overview of potential protein-protein interaction pattern in the sarcolemma-enriched fraction from *mdx-4cv* skeletal muscle. In order to identify potential protein-protein interaction pattern of decreased (a) and increased (b) proteins in the sarcolemma fraction from *mdx-4cv* muscle (Tables 1, 2 and S1), the bioinformatics software programme STRING was

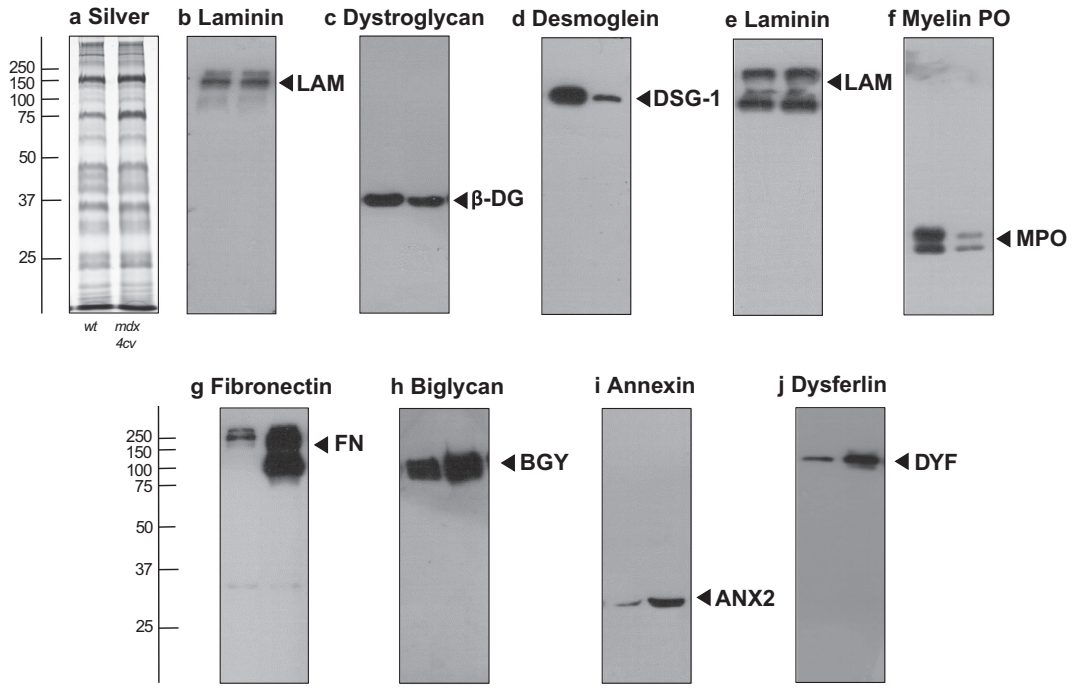

Fig. 4. Immunoblot analysis of altered sarcolemma-associated proteins in dystrophin-deficient *mdx-4cv* skeletal muscle extracts. Shown is a silver-stained gel (a) and corresponding immunoblots labelled with antibodies to the basal lamina component laminin (LAM; b,e), β-dystroglycan (β-DG; c), the cytolinker desmoglein isoform 1 (DSG1; d), myelin PO protein (MPO; f), fibronectin (FN; g), biglycan (BYG; h), annexin A2 (ANX2; i) and dysferlin (DYS; j). Lanes 1 and 2 represent 5-month old wild type (*wt*) versus age-matched *mdx-4cv* hind limb muscle extracts, respectively. In panels (e) and (f), 50 μg protein/lane, and in all other panels 25 μg protein/lane were loaded. Molecular mass standards are marked on the left of panels. The comparative immunoblotting of laminin (k, n), β-dystroglycan (l), the cytolinker desmoglein isoform 1 (m), myelin PO protein (o), fibronectin (p), biglycan (q), annexin A2 (r) and dysferlin (s) between crude extracts from wild type versus *mdx-4cv* mice was statistically evaluated using an unpaired Student's *t*-test (Mean values ± SEM; $n = 4$; $^{*}p < 0.05$; $^{**}p < 0.01$; $^{***}p < 0.001$).

proteins with a changed abundance in *mdx-4cv* muscles and previously established markers of muscular dystrophy-related alteration in protein expression levels. Silver-staining of a representative gel indicated no major differences in protein banding patterns between crude wild type versus *mdx-4cv* preparations (Fig. 4a). As a control of a major protein species that exhibits no significant changes in its abundance, the immunoblotting of laminin is shown for protein loading of 25 μg and 50 μg per lane (Fig. 4b, e). The established dystrophin-associated glycoprotein β-dystroglycan and the recently described cytolinker protein desmoglein isoform DSG-1 were both confirmed to be reduced in muscular dystrophy (Fig. 4c,d), establishing the mutant status of the *mdx-4cv* muscle preparations used in this study. Importantly, the mass spectrometrically identified myelin PO protein was verified to be of lower concentration in dystrophinopathy (Fig. 4f). In analogy, increases in the extracellular matrix component fibronectin, the dystrophin-associated protein biglycan, the annexin isoform ANX2 and the newly identified protein dysferlin were confirmed by immunoblotting (Fig. 4g–j). Fig. 4k–s summarizes the statistical evaluation of the immunoblot analysis shown in Fig. 4a–j.

3.5. Immunofluorescence microscopy of dystrophic mdx-4cv skeletal muscle tissue

The histopathological and mutant status of *mdx-4cv* mouse muscles were verified by hematoxylin/eosin staining and the immunofluorescence microscopical analysis of the full-length Dp427-M isoform of dystrophin, respectively. Fig. 5a–d clearly shows that the *mdx-4cv gastrocnemius* muscle is almost completely lacking dystrophin at its surface membrane and that the dystrophic phenotype is associated with the presence of central nucleation, considerable variations in fibre diameter and apparent fibrosis and inflammation. The analysis of myoferlin expression using transverse cryosections of *soleus* and diaphragm muscles confirmed the results from the proteomic survey of the dystrophin-deficient sarcolemma. Myoferlin was shown to exist at a higher concentration in slow *soleus* and severely dystrophic diaphragm muscle from the *mdx-4cv* mouse, as compared to wild type (Fig. 5e–l). The immunofluorescence labelling of myoferlin in *gastrocnemius* and *tibialis anterior* muscle specimens showed relatively poor specific staining patterns (not shown) and was not further pursued. In wild type *soleus* and diaphragm muscles, myoferlin is probably mostly present in degenerating fibres, and drastically up-regulated in the dystrophic phenotype.

4. Discussion

The almost complete loss of dystrophin isoform Dp427-M causes a plethora of secondary changes in dystrophic skeletal muscles that negatively affect many cellular processes, physiological mechanisms and biochemical pathways [51]. Under healthy conditions, contractile force is transmitted between sarcomeric *Z*-disks and M-lines of myofibrils and bridged across the sarcolemma towards the extracellular matrix and the tendon structure. The lack of the dystrophin lattice as a molecular anchor and scaffold weakens this crucial structural linkage between the intracellular cytoskeleton and the extracellular collagen assembly, which results in impaired lateral force transmission in dystrophic muscle fibres [52]. The proteomic profiling of the sarcolemma-enriched fraction from hind limb muscles of the *mdx-4cv* mouse model of dystrophinopathy presented here confirms this highly complex pathophysiology [53,54]. Distinct changes in the dystrophin-deficient plasma membrane agree with the idea of multifaceted secondary alterations due to the primary abnormality in the sub-sarcolemmal cytoskeleton, as summarized in Fig. 6. As compared to previous proteomic surveys of dystrophic muscle tissues [21–23], this systematic analysis with a focus on the sarcolemmal membrane system and its associated intra- and extracellular structures has identified interesting new protein alterations, as well as confirmed critical pathobiochemical mechanisms of

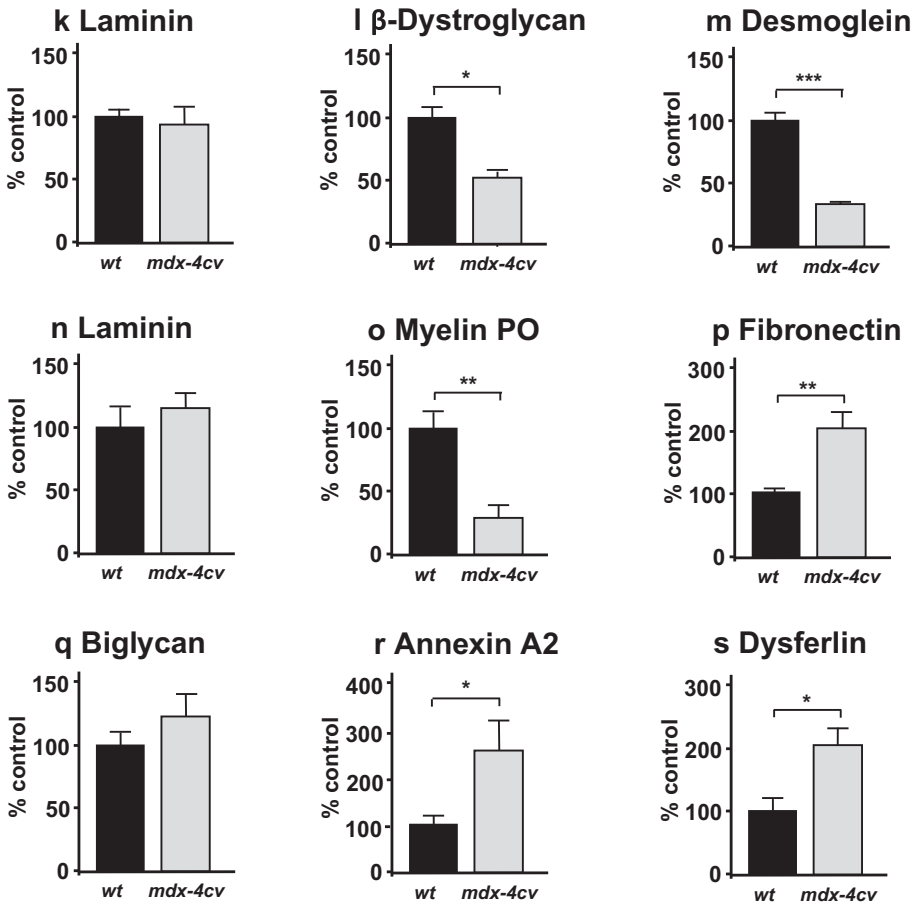

Fig. 4. (*continued*)

muscular dystrophy.

Proteome-wide changes associated with muscular dystrophy include significant alterations in noteworthy protein species involved in plasmalemmal repair, cellular signalling, ion handling, innervation, fibre regeneration, protein synthesis, the excitation-contraction-relaxation cycle, energy metabolism, metabolite transportation, the innate immune response, the cytoskeletal network and the extracellular matrix. Large-scale profiling approaches using comparative organellar proteomics are usually complicated by both technical and biological issues [55–57]. In the case of the muscle surface membrane isolated from mutant mouse hind limb homogenates, the following bioanalytical obstacles should therefore be taken into account during the interpretation and extrapolation of mass spectrometric findings: (i) the sarcolemmal subproteome embodies only a small percentage of the constituents of the entire skeletal muscle proteome, therefore requiring the pooling of individual subtypes of slow, mixed and fast muscles for the initial proteomic screening procedure, (ii) skeletal muscle tissues are heterogeneous in composition and contain besides various types of extrafusal contractile fibres also motor neurons, immune cells, capillaries, satellite cells, muscle spindles and several complex layers of connective tissue and tendons, and (iii) subcellular fractionation protocols for the enrichment of the plasmalemma membrane that employ differential centrifugation and affinity agglutination approaches, are often complicated by a considerable amount of cross-contamination due to protein desorption, adsorption and vesicular entrapment [56]. If these analytical issues are properly considered, the subproteomic analysis of the enriched plasmalemma can be highly useful, since it encompasses the crucial advantage of firmly reducing sample complexity. This should decisively improve the coverage of protein species belonging to the sarcolemma-cytoskeleton-extracellular matrix axis of the skeletal muscle periphery.

The proteomic profiling of the *mdx-4cv* sarcolemma clearly confirmed dystrophin as the most drastically decreased protein in muscular dystrophy and the concomitant reduction in the expression of the core members of the dystrophin-associated glycoprotein complex, i.e. dystroglycans and sarcoglycans [8]. Immunoblotting also confirmed the lower concentration of β-dystroglycan and the dystrophin-associated cytolinker desmoglein [38]. In contrast, isoforms of the plasma membrane scaffolding protein flotillin, which is closely associated with caveolin-3 within caveolar membranes that are void of the dystrophin-complex [58], was shown to be increased in the Dp427-deficient sarcolemma. An interesting new aspect of the muscular dystrophy-initiating disintegration of the dystrophin complex is the identification of a reduced expression of the heteropolymeric intermediate filament protein synemin, which was previously shown to be linked to dystrophin and utrophin [37]. In contrast to synemin, the indirectly dystrophin-linked proteins vimentin and tubulin are increased in *mdx-4cv* muscle and this probably represents compensatory processes to rescue the dystrophin-lacking cytoskeleton [18,43]. In skeletal muscle fibres, cytoplasmic synemin is associated with desmin and vimentin filaments and thereby contributes to cellular resilience by supporting cell shape, adhesion and migration [59]. Synemin and its association with the intermediate filament network strengthens the linkage between myofibrils and sarcolemmal costamers, as well as the plasmalemma region at the neuromuscular and myotendinous junctions. Since intermediate filaments surround the *Z*-lines, this cytoskeletal structure links sarcomeric units of myofibrils to costameres and provides mechanical stability to contractile cells [2]. Hence, reduced levels of synemin may play a central role in the secondary pathobiochemical changes that render dystrophin-deficient fibres more susceptible to micro-rupturing

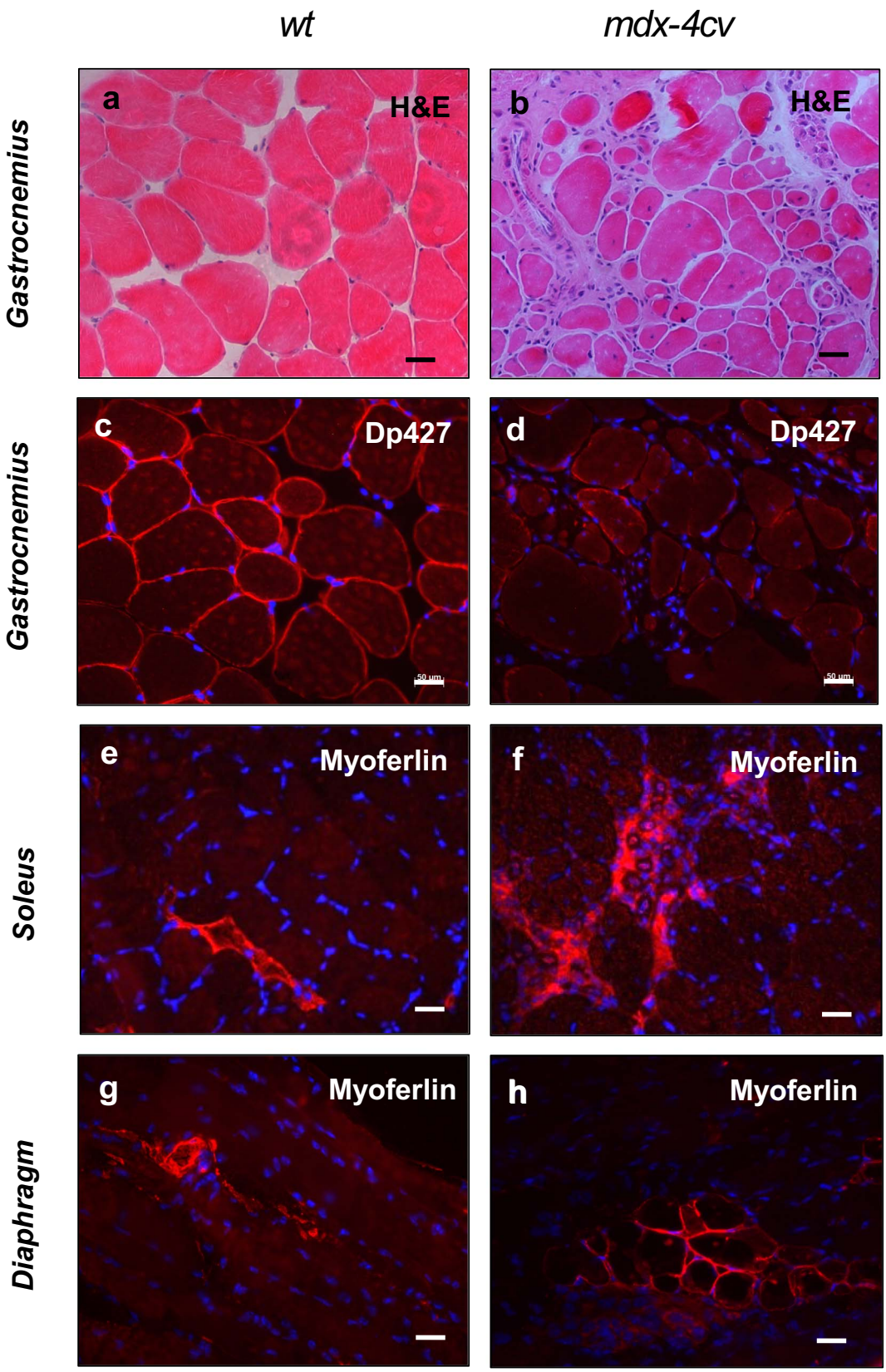

Fig. 5. Histological and immunofluorescence microscopical analysis of dystrophic *mdx-4cv* skeletal muscle. Shown are transverse sections of *gastrocnemius* (a–d), *soleus* (e, f) and diaphragm (g, h) muscles from 6-month old wild type (a, c, e, g; *wt*) and dystrophic (b, d, f, h; *mdx-4cv*) mice. Cryosections were stained with hematoxylin and eosin (H&E; a, b), as well as immuno-labelled with antibodies to the full-length dystrophin isoform Dp427 (c, d) and myoferlin (e–h). Bar equals 50 μm.

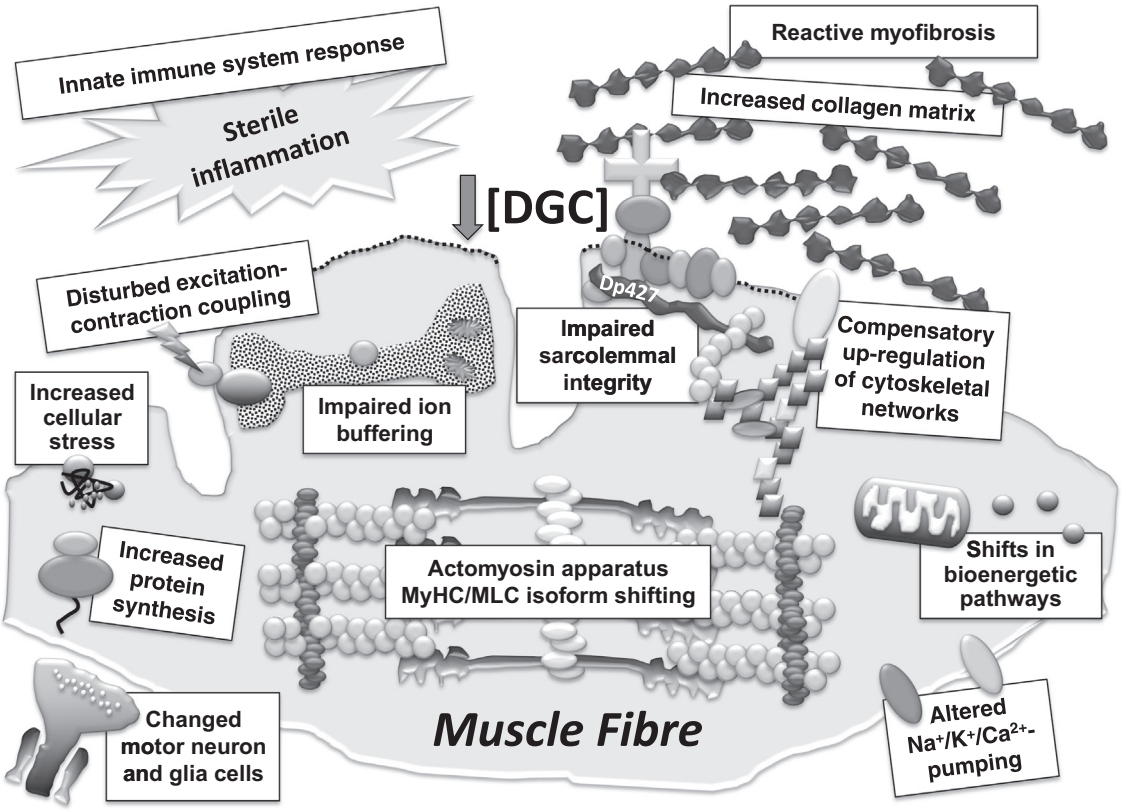

Fig. 6. Diagrammatic summary of altered subcellular processes in dystrophic *mdx-4cv* skeletal muscle as revealed from the proteomic profiling of a sarcolemma-enriched fraction.

of the disintegrating sarcolemma.

The potentially impaired linkage of synemin to the sub-sarcolemmal cytoskeleton of the neuromuscular junction [59] is an interesting result in connection with the identified reduction of myelin protein PO and periaxin. Myelin protein PO is crucial for the maintenance and functionality of peripheral myelin, and the scaffolding protein periaxin is an integral member of the dystroglycan complex in Schwann cells, which also contains the dystrophin-related protein isoform DRP2 [60]. Lower levels of these glia cell components indicate muscular dystrophy-related changes in the motor neuron system especially related to peripheral nerve myelination, and agree with the previously described remodelling of both pre- and postsynaptic regions of the neuromuscular junction during dystrophic progression [61]. In contrast to Schwann cell markers, the neural cell adhesion molecule NCAM1 and the synaptic vesicle membrane protein VAT1 were shown to be increased in the sarcolemma-enriched fraction from dystrophic muscle. The VAT1 protein is involved in vesicular transport and important for the overall process of neurotransmitter storage and release at cholinergic synapses. In mature skeletal muscle, NCAM1 is mostly located at the motor endplate and not the sarcolemma [62], but its expression increases during muscle fibre regeneration [63]. Thus, the occurrence of elevated NCAM1 levels would match the concept of adaptive process in the dystrophic phenotype and degeneration-regeneration cycles in the neuromuscular system [64].

Fibre regeneration, muscle adaptations, an enhanced cellular stress response and membrane reestablishment, as well as the activation of the innate immune system, are in agreement with the proteomic identification of drastically increased proteins belonging to the ferlin and annexin family of repair proteins, immune cell markers, molecular chaperones and ribosomal components. The considerable levels of 40S and 60S ribosomal proteins involved in protein synthesis is indicative of major regenerative processes occurring during repair cycles in dystrophic muscle tissue. The enrichment in ribosomal components is most likely not due to direct interactions of ribosomes with the sarcolemma, but more likely due to the fact that the sarcolemma-enriched fraction contains a high degree of cross-contamination from other organelles and membrane systems. However, although an immunohistological study indicates that ribosomes are majorly located in the inter-myofibrillar cytoplasm, they appear to also reside in the sub-sarcolemmal space in skeletal muscle fibres [65]. Myoferlin, dysferlin and annexins, in conjunction with the stabilising effect of the cortical actin cytoskeleton, are critical factors in muscle membrane fusion events and the Ca^{2+}- and membrane injury-related repair of the sarcolemma [66–68]. Dysferlin and myoferlin also regulate transverse tubule formation and Ca^{2+}-homeostasis, making them crucial players in the establishment of the fibre periphery, its membrane invaginations and ion regulation [69,70]. Plasma membrane repair and efficient resealing are essential protective mechanisms for the swift recovery from fibre injury [71]. The proteomic establishment of elevated levels of myoferlin [18] and its closely related isoform dysferlin agree with previous cell biological studies on membrane repair and vesicle wound patching in muscular dystrophy [72,73]. The identification of increases in annexin A1 [74] supports the previous demonstration that annexins are universal markers of dystrophinopathy [43]. Hence, the increased concentration of myoferlin, dysferlin and the Ca^{2+}-triggered phospholipid-binding isoform A1 of annexin in the dystrophin-deficient sarcolemma strongly indicates plasmalemmal wound-healing to counteract detrimental membrane rupturing. Annexin A1 is also a critical factor for the restoration of cellular homeostasis by modulating the inflammatory response [75].

Increased levels of inflammatory modifiers are in line with the finding that the protein species with the most highly elevated concentration in the sarcolemma-enriched fraction from *mdx-4cv* muscle are markers of immune cells, including eosinophil peroxidase [76], subunits of the histocompatibility complex [77] and receptor-type tyrosine-protein phosphatase C, which is a positive regulator of T-cell co-activation [78]. In addition, other immune cell markers included sialoadhesin and macrophage mannose receptor. Interestingly, the 60-

fold increased caspase recruitment domain-containing protein Card19 was previously shown to counteract the activating effects of the protein Blc10 on the nuclear factor NF-kappa-B and its central role in innate immunity [79]. Cellular immune responses and sterile inflammation clearly contribute to muscular changes in dystrophinopathy [80–82]. However, it is not fully understood whether the inflammatory process in degenerating muscles is mostly due to a pathophysiological mechanism that promotes fibre wasting independent of sarcolemmal rupturing, or if it is based on the relatively non-specific and reactive invasion of macrophages and other immune cells in necrotic muscle cells [83,84]. Importantly, serum analyses of dystrophinopathy showed increased levels of the acute phase response plasma marker haptoglobin [85], which is a robust indicator of tissue damage-induced inflammation [45]. Thus, the proteomic identification of immune cell markers in the sarcolemma fraction from dystrophic muscles supports the concept that immune cell infiltration is a key feature of degenerating muscle fibres in Duchenne muscular dystrophy [86].

In agreement with previous proteomic studies of the severely fibrotic *mdx* diaphragm muscle [14], young *mdx* hind limb muscles during the acute phase of Dp427 deficiency [87] and the moderately dystrophic *mdx quadriceps femoris* muscle [38], this report confirmed that lack of dystrophin triggers an enhanced cellular stress response in dystrophic fibres. Molecular chaperone activities are essential for the safeguarding of proteostasis by averting cytotoxic levels of detrimental protein aggregation. This is achieved by promoting the efficient removal of irreversibly misfolded protein structures, as well as the initiation of refolding to stabilise compromised, but salvageable proteins. A variety of stress proteins, including the heat shock proteins HSPB5, HSPB7, HSPA and HSPC are elevated in dystrophic muscles and promote accelerated peptide folding to support skeletal muscle proteins to resume their proper functional fold [88]. The increased expression of the small heat shock protein HSPB1 of 27 kDa, the collagen-specific molecular chaperone HSP47 (serpin H1) and the enzyme protein-disulfide isomerase, as determined here by comparative proteomics, illustrates that molecular chaperones play an important role in the prevention of proteotoxic side effects in dystrophinopathy.

In the adult skeletal musculature, the ratio of slow, fast and hybrid fibres relate to the functional demands of individual muscle subtypes. Distinct shifts in fibre types correlate usually with concomitant changes in the density or isoform expression pattern of the main protein species involved in the contraction-relaxation cycle, bioenergetic pathways, cellular signalling complexes and the Ca^{2+}-handling apparatus. As reviewed by Dowling et al. [89], clear fibre type shifting is observed in individual skeletal muscles during drastic changes in body weight, diabetes mellitus, cancer cachexia, disuse atrophy, motor neuron disease, myotonia, inflammatory myopathies, autoimmune muscle diseases, myofibrillar myopathies and age-related muscle wasting. In the many forms of muscular dystrophy, moderate fibre type conversions occur whereby slow-twitching fibre populations have a tendency to undergo degenerative processes later than fast type IIb fibres in dystrophinopathy [90]. Remarkably, one-quarter of all fibres in Duchenne patients exhibit only the adult slow isoform of myosin heavy chain, whereby the disruption of MyHC gene switching between the mature fast and slow MyHC isoforms coincides with the deletion in dystrophin [91]. Previous proteomic studies indicate moderate alteration in the isoform expression patterns of myosin, actin, actinin, myozenin, myomesin, tropomyosin and troponin [14–16,18,87,92,93]. In this study focusing on the sarcolemma-enriched fraction, co-purifying proteins derived from the sarcomere, sarcoplasmic reticulum, mitochondria and cytosol of dystrophic fibres revealed some impact on fibre specification. This included increases in contractile myosin heavy chains MyHC-2×, MyHC-2b and embryonic myosin-3, as well as cellular myosin-9, α-actinin-1 and fast myosin-binding protein C [94]. Mitochondrial proteins are differentially expressed in *mdx-4cv* muscles with complex changes in many enzymes and metabolite carriers involved in bioenergetics and regulatory processes, including pyruvate dehydrogenase, NADH dehydrogenase, ATP synthase, metalloendopeptidase, ADP/ATP translocase, Ca^{2+}-uniporter, ferrochelatase and aldehyde dehydrogenase. The glycolytic enzymes phosphoglycerate kinase and aldolase were shown to be reduced in dystrophic muscle [95]. These results demonstrate complex changes in bioenergetic pathways and the contraction-relaxation cycle, but no clear fibre type switching that involves parallel changes in metabolism and contraction kinetics.

In support of previous findings on altered excitation-contraction coupling and impaired ion handling in dystrophinopathy, this study confirmed altered levels of certain isoforms of Ca^{2+}-channels, Ca^{2+}-ATPases and luminal Ca^{2+}-binding proteins. There appears to be a switch in the slow CSQ2 and fast CSQ1 isoform of the Ca^{2+}-buffering protein calsequestrin of the terminal cisternae region [96], a reduction in the Ca^{2+}-shuttle protein sarcalumenin of the longitudinal tubules [97], a lower concentration of the β-subunit of the voltage-sensing L-type Ca^{2+}-channel of the transverse tubules, and apparent increases in the ryanodine receptor Ca^{2+}-release channel of the triad junction, the slow SERCA2 Ca^{2+}-pump of the sarcoplasmic reticulum, the sarcolemmal PMCA-type Ca^{2+}-ATPase, and the stromal interaction molecule Stim1 that activates store-operated Ca^{2+}-channels in the plasma membrane. These changes in major Ca^{2+}-handling proteins reflect the central pathophysiological role of abnormal ion fluxes in muscular dystrophy, which is linked to the chronic influx of Ca^{2+}-ions through the leaky plasma membrane, elevated cytosolic Ca^{2+}-levels triggering proteolytic degradation cycles and an impaired luminal Ca^{2+}-buffering capacity in dystrophic muscle fibres [51,53]. In addition, up-regulation of the sarcolemmal Na^+/K^+-ATPase in damaged fibres indicates a compensatory mechanism in muscular dystrophy that attempts to normalise aberrant cation fluxes and thereby stabilise the membrane potential over the dystrophin-deficient sarcolemma [18,98].

Besides progressive fibre wasting, sterile inflammation and cellular stress, another key feature of the dystrophic phenotype is reactive myofibrosis [99]. In contrast to the dystrophin-deficient and fibrotic heart muscle [44], the expression of the basal lamina component laminin-211 is unchanged in dystrophic skeletal muscle, which was also shown here by immunoblotting. However, the current study shows that integrins exhibit differential concentration changes, possibly as a compensatory mechanism to counteract the loss of the dystrophin-dystroglycan linkage to the basal lamina. Higher levels of extracellular matrix proteins were previously described in a variety of proteomic studies, including dermatopontin, periostin, mimecan, asporin, decorin, fibronectin, collagen I and collagen VI [16,20,43,100]. The analysis of the sarcolemma membrane system from the dystrophic *mdx-4cv* mouse showed an increased concentration in biglycan, fibronectin, vitronectin and the collagen COL α-1 and COL α-2 VI-chains, which agrees with previous biochemical investigations into muscular dystrophy-related myofibrosis [22]. The observed muscular dystrophy-associated turnover within the complex collagen system of the extracellular matrix is also evident by the identification of an increased concentration of the collagen-specific molecular chaperone named serpin H1, which is more commonly classified as heat shock protein HSP47 [101]. HSP47 plays a key role in collagen biosynthesis. High levels of collagens and other extracellular matrix proteins cause progressive tissue scarring resulting in a critical loss of muscle elasticity [22], and therefore probably play a central role in the secondary abnormalities of X-linked muscular dystrophy [99].

5. Conclusion

X-linked muscular dystrophy is a highly complex neuromuscular disorder with intricate pathophysiological changes and compensatory adaptations on the molecular and cellular level. Dystrophinopathy is characterized by progressive fibre degeneration, fatty tissue replacement, reactive myofibrosis and sterile inflammation. Previous proteomic studies have confirmed complex changes in a variety of protein families involved in muscle contraction, cellular signalling, energy

metabolism, ion handling and the stress response. Based on these findings, an organellar proteomic profiling survey was initiated with a focus on the sarcolemma membrane and its associated intra- and extracellular structures. Subproteomic results were analysed by bioinformatics and key findings confirmed by immunoblotting and immunofluorescence microscopy. Dystrophin and its tightly associated glycoproteins were shown to be greatly reduced, as well as the intermediate filament component synemin. In contrast, the extracellular dystrophin complex-linked proteoglycan biglycan and the cytoskeletal element vimentin exhibited an increased abundance in dystrophin-deficient muscles, probably representing compensatory mechanisms. The initiation of membrane repair processes and increased protein synthesis was indicated by high levels of myoferlin, dysferlin and annexin A1, and various ribosomal protein subunits, respectively. Interestingly, reductions in the scaffolding protein periaxin and myelin PO protein of Schwann cells suggest changed myelination levels of motor neurons in muscular dystrophy. Besides confirming changes in metabolic pathways, disturbed ion homeostasis, increased levels of molecular chaperones and collagen deposition related to myofibrosis, the analysis of the sarcolemma established considerable levels of invading immune cells, which agrees with a highly active innate immune system in muscular dystrophy.

Acknowledgments

Research was supported by a Hume scholarship from Maynooth University, and project grants from Muscular Dystrophy Ireland and the Irish Health Research Board (HRB/MRCG-2016-20). The Q-Exactive quantitative mass spectrometer was funded under the Research Infrastructure Call 2012 by Science Foundation Ireland (SFI-12/RI/2346/3). The authors would like to thank Ms. Caroline Batchelor for expert technical support with mass spectrometry.

Conflicts of interest statement

The authors certify that they have NO affiliations with or involvement in any organization or entity with any financial interest (such as honoraria; educational grants; participation in speakers' bureaus; membership, employment, consultancies, stock ownership, or other equity interest; and expert testimony or patent-licensing arrangements), or non-financial interest (such as personal or professional relationships, affiliations, knowledge or beliefs) in the subject matter or materials discussed in this manuscript.

References

[1] A.K. Peter, H. Cheng, R.S. Ross, K.U. Knowlton, J. Chen, The costamere bridges sarcomeres to the sarcolemma in striated muscle, Prog. Pediatr. Cardiol. 31 (2011) 83–88.
[2] M. Gautel, K. Djinović-Carugo, The sarcomeric cytoskeleton: from molecules to motion, J. Exp. Biol. 219 (2016) 135–145.
[3] C.A. Henderson, C.G. Gomez, S.M. Novak, L. Mi-Mi, C.C. Gregorio, Overview of the muscle cytoskeleton, Compr. Physiol. 7 (2017) 891–944.
[4] O. Jaka, L. Casas-Fraile, A. López de Munain, A. Sáenz, Costamere proteins and their involvement in myopathic processes, Expert Rev. Mol. Med. 17 (2015) e12.
[5] J.C. Calderón, P. Bolaños, C. Caputo, The excitation-contraction coupling mechanism in skeletal muscle, Biophys. Rev. 6 (2014) 133–160.
[6] E.P. Hoffman, R.H. Brown Jr., L.M. Kunkel, Dystrophin: the protein product of the Duchenne muscular dystrophy locus, Cell 51 (1987) 919–928.
[7] K.F. O'Brien, L.M. Kunkel, Dystrophin and muscular dystrophy: past, present, and future, Mol. Genet. Metab. 74 (2001) 75–88.
[8] J.M. Ervasti, K. Ohlendieck, S.D. Kahl, M.G. Gaver, K.P. Campbell, Deficiency of a glycoprotein component of the dystrophin complex in dystrophic muscle, Nature 345 (1990) 315–319.
[9] K. Ohlendieck, Towards an understanding of the dystrophin-glycoprotein complex: linkage between the extracellular matrix and the membrane cytoskeleton in muscle fibers, Eur. J. Cell Biol. 69 (1996) 1–10.
[10] B. Constantin, Dystrophin complex functions as a scaffold for signalling proteins, Biochim. Biophys. Acta 1838 (2014) 635–642.
[11] K. Ohlendieck, K. Matsumura, V.V. Ionasescu, J.A. Towbin, E.P. Bosch, S.L. Weinstein, S.W. Sernett, K.P. Campbell, Duchenne muscular dystrophy: deficiency of dystrophin-associated proteins in the sarcolemma, Neurology 43 (1993) 795–800.
[12] A. Holland, S. Carberry, K. Ohlendieck, Proteomics of the dystrophin-glycoprotein complex and dystrophinopathy, Curr. Protein Pept. Sci. 14 (2013) 680–697.
[13] Y. Ge, M.P. Molloy, J.S. Chamberlain, P.C. Andrews, Proteomic analysis of mdx skeletal muscle: great reduction of adenylate kinase 1 expression and enzymatic activity, Proteomics 3 (2003) 1895–1903.
[14] P. Doran, G. Martin, P. Dowling, H. Jockusch, K. Ohlendieck, Proteome analysis of the dystrophin-deficient MDX diaphragm reveals a drastic increase in the heat shock protein cvHSP, Proteomics 6 (2006) 4610–4621.
[15] S. Rayavarapu, W. Coley, E. Cakir, V. Jahnke, S. Takeda, Y. Aoki, H. Grodish-Dressman, J.K. Jaiswal, E.P. Hoffman, K.J. Brown, Y. Hathout, K. Nagaraju, Identification of disease specific pathways using in vivo SILAC proteomics in dystrophin deficient mdx mouse, Mol. Cell. Proteomics 12 (2013) 1061–1073.
[16] A. Holland, P. Dowling, P. Meleady, M. Henry, M. Zweyer, R.R. Mundegar, D. Swandulla, K. Ohlendieck, Label-free mass spectrometric analysis of the mdx-4cv diaphragm identifies the matricellular protein periostin as a potential factor involved in dystrophinopathy-related fibrosis, Proteomics 15 (2015) 2318–2331.
[17] A.M. Coenen-Stass, G. McClorey, R. Manzano, C.A. Betts, A. Blain, A.F. Saleh, M.J. Gait, H. Lochmüller, M.J. Wood, T.C. Roberts, Identification of novel, therapy-responsive protein biomarkers in a mouse model of Duchenne muscular dystrophy by aptamer-based serum proteomics, Sci. Rep. 5 (2015) 17014.
[18] S. Murphy, M. Henry, P. Meleady, M. Zweyer, R.R. Mundegar, D. Swandulla, K. Ohlendieck, Simultaneous pathoproteomic evaluation of the dystrophin-glycoprotein complex and secondary changes in the mdx-4cv mouse model of Duchenne muscular dystrophy, Biology (Basel) 4 (2015) 397–423.
[19] T.C. Roberts, H.J. Johansson, G. McClorey, C. Godfrey, K.E. Blomberg, T. Coursindel, M.J. Gait, C.I. Smith, J. Lehtiö, S. El Andaloussi, M.J. Wood, Multi-level omics analysis in a murine model of dystrophin loss and therapeutic restoration, Hum. Mol. Genet. 24 (2015) 6756–6768.
[20] S. Murphy, M. Zweyer, R.R. Mundegar, M. Henry, P. Meleady, D. Swandulla, K. Ohlendieck, Concurrent label-free mass spectrometric analysis of dystrophin isoform Dp427 and the myofibrosis marker collagen in crude extracts from mdx-4cv skeletal muscles, Proteomes 3 (2015) 298–327.
[21] H.R. Fuller, L.C. Graham, M. Llavero Hurtado, T.M. Wishart, Understanding the molecular consequences of inherited muscular dystrophies: advancements through proteomic experimentation, Expert Rev. Proteomics 13 (2016) 659–671.
[22] A. Holland, S. Murphy, P. Dowling, K. Ohlendieck, Pathoproteomic profiling of the skeletal muscle matrisome in dystrophinopathy associated myofibrosis, Proteomics 16 (2016) 345–366.
[23] S.J. Carr, R.P. Zahedi, H. Lochmüller, A. Roos, Mass spectrometry-based protein analysis to unravel the tissue pathophysiology in Duchenne muscular dystrophy, Proteomics Clin. Appl. (Jun 20 2017), http://dx.doi.org/10.1002/prca.201700071.
[24] J.H. Shin, C.H. Hakim, K. Zhang, D. Duan, Genotyping mdx, mdx3cv, and mdx4cv mice by primer competition polymerase chain reaction, Muscle Nerve 43 (2011) 283–286.
[25] I. Danko, V. Chapman, J.A. Wolff, The frequency of revertants in mdx mouse genetic models for Duchenne muscular dystrophy, Pediatr. Res. 32 (1992) 128–131.
[26] T.A. Partridge, The mdx mouse model as a surrogate for Duchenne muscular dystrophy, FEBS J. 280 (2013) 4177–4186.
[27] S. Murphy, K. Ohlendieck, Mass spectrometric identification of dystrophin, the protein product of the Duchenne muscular dystrophy gene, in distinct muscle surface membranes, Int. J. Mol. Med. 40 (2017) 1078–1088.
[28] K. Ohlendieck, J.M. Ervasti, J.B. Snook, K.P. Campbell, Dystrophin-glycoprotein complex is highly enriched in isolated skeletal muscle sarcolemma, J. Cell Biol. 112 (1991) 135–148.
[29] A.S. Deshmukh, M. Murgia, N. Nagaraj, J.T. Treebak, J. Cox, M. Mann, Deep proteomics of mouse skeletal muscle enables quantitation of protein isoforms, metabolic pathways, and transcription factors, Mol. Cell. Proteomics 14 (2015) 841–853.
[30] S. Murphy, K. Ohlendieck, The biochemical and mass spectrometric profiling of the dystrophin complexome from skeletal muscle, Comput. Struct. Biotechnol. J. 14 (2015) 20–27.
[31] C. Lewis, K. Ohlendieck, Mass spectrometric identification of dystrophin isoform Dp427 by on-membrane digestion of sarcolemma from skeletal muscle, Anal. Biochem. 404 (2010) 197–203.
[32] J.H. Yoon, E. Johnson, R. Xu, L.T. Martin, P.T. Martin, F. Montanaro, Comparative proteomic profiling of dystroglycan-associated proteins in wild type, mdx, and Galgt2 transgenic mouse skeletal muscle, J. Proteome Res. 11 (2012) 4413–4424.
[33] R. Turk, J.J. Hsiao, M.M. Smits, B.H. Ng, T.C. Pospisil, K.S. Jones, K.P. Campbell, M.E. Wright, Molecular signatures of membrane protein complexes underlying muscular dystrophy, Mol. Cell. Proteomics 15 (2016) 2169–2185.
[34] J.E. Brenman, D.S. Chao, H. Xia, K. Aldape, D.S. Bredt, Nitric oxide synthase complexed with dystrophin and absent from skeletal muscle sarcolemma in Duchenne muscular dystrophy, Cell 82 (1995) 743–752.
[35] M.A. Bowe, D.B. Mendis, J.R. Fallon, The small leucine-rich repeat proteoglycan biglycan binds to alpha-dystroglycan and is upregulated in dystrophic muscle, J. Cell Biol. 148 (2000) 801–810.
[36] M.R. Stone, A. O'Neill, D. Catino, R.J. Bloch, Specific interaction of the actin-binding domain of dystrophin with intermediate filaments containing keratin 19, Mol. Biol. Cell 16 (2005) 4280–4293.
[37] R.C. Bhosle, D.E. Michele, K.P. Campbell, Z. Li, R.M. Robson, Interactions of intermediate filament protein synemin with dystrophin and utrophin, Biochem. Biophys. Res. Commun. 346 (2006) 768–777.

[38] S. Murphy, H. Brinkmeier, M. Krautwald, M. Henry, P. Meleady, K. Ohlendieck, Proteomic profiling of the dystrophin complex and membrane fraction from dystrophic mdx muscle reveals decreases in the cytolinker desmoglein and increases in the extracellular matrix stabilizers biglycan and fibronectin, J. Muscle Res. Cell Motil. 38 (2017) 251–268.
[39] V.M. Chapman, D.R. Miller, D. Armstrong, C.T. Caskey, Recovery of induced mutations for X chromosome-linked muscular dystrophy in mice, Proc. Natl. Acad. Sci. U. S. A. 86 (1989) 1292–1296.
[40] S. Carberry, M. Zweyer, D. Swandulla, K. Ohlendieck, Comparative proteomic analysis of the contractile-protein-depleted fraction from normal versus dystrophic skeletal muscle, Anal. Biochem. 446 (2014) 108–115.
[41] K. Ohlendieck, Characterisation of the dystrophin-related protein utrophin in highly purified skeletal muscle sarcolemma vesicles, Biochim. Biophys. Acta 1283 (1996) 215–222.
[42] M.M. Bradford, A rapid and sensitive method for the quantitation of microgram quantities of protein utilizing the principle of protein-dye binding, Anal. Biochem. 72 (1976) 248–254.
[43] A. Holland, M. Henry, P. Meleady, C.K. Winkler, M. Krautwald, H. Brinkmeier, K. Ohlendieck, Comparative label-free mass spectrometric analysis of mildly versus severely affected mdx mouse skeletal muscles identifies annexin, lamin, and vimentin as universal dystrophic markers, Molecules 20 (2015) 11317–11344.
[44] S. Murphy, P. Dowling, M. Zweyer, R.R. Mundegar, M. Henry, P. Meleady, D. Swandulla, K. Ohlendieck, Proteomic analysis of dystrophin deficiency and associated changes in the aged mdx-4cv heart model of dystrophinopathy-related cardiomyopathy, J. Proteome 145 (2016) 24–36.
[45] S. Murphy, P. Dowling, M. Zweyer, M. Henry, P. Meleady, R.R. Mundegar, D. Swandulla, K. Ohlendieck, Proteomic profiling of mdx-4cv serum reveals highly elevated levels of the inflammation-induced plasma marker haptoglobin in muscular dystrophy, Int. J. Mol. Med. 39 (2017) 1357–1370.
[46] K.R. Ting, M. Henry, J. Meiller, A. Larkin, M. Clynes, P. Meleady, D. Bazou, P. Dowling, P. O'Gorman, Novel panel of protein biomarkers to predict response to bortezomib-containing induction regimens in multiple myeloma patients, BBA Clin 8 (2017) 28–34.
[47] S. Murphy, M. Zweyer, M. Henry, P. Meleady, R.R. Mundegar, D. Swandulla, K. Ohlendieck, Label-free mass spectrometric analysis reveals complex changes in the brain proteome from the mdx-4cv mouse model of Duchenne muscular dystrophy, Clin. Proteomics 12 (2015) 27.
[48] R.R. Mundegar, E. Franke, R. Schäfer, M. Zweyer, A. Wernig, Reduction of high background staining by heating unfixed mouse skeletal muscle tissue sections allows for detection of thermostable antigens with murine monoclonal antibodies, J. Histochem. Cytochem. 56 (2008) 969–975.
[49] K. Ohlendieck, K.P. Campbell, Dystrophin constitutes 5% of membrane cytoskeleton in skeletal muscle, FEBS Lett. 283 (1991) 230–234.
[50] S. Murphy, P. Dowling, M. Zweyer, R.R. Mundegar, M. Henry, P. Meleady, D. Swandulla, K. Ohlendieck, Subproteomic profiling of sarcolemma from dystrophic mdx-4cv skeletal muscle, Data Brief (2018) (submitted).
[51] D.G. Allen, N.P. Whitehead, S.C. Froehner, Absence of dystrophin disrupts skeletal muscle signaling: roles of Ca^{2+}, reactive oxygen species, and nitric oxide in the development of muscular dystrophy, Physiol. Rev. 96 (2016) 253–305.
[52] K.S. Ramaswamy, M.L. Palmer, J.H. van der Meulen, A. Renoux, T.Y. Kostrominova, D.E. Michele, J.A. Faulkner, Lateral transmission of force is impaired in skeletal muscles of dystrophic mice and very old rats, J. Physiol. 589 (2011) 1195–1208.
[53] F.W. Hopf, P.R. Turner, R.A. Steinhardt, Calcium misregulation and the pathogenesis of muscular dystrophy, Subcell. Biochem. 45 (2007) 429–464.
[54] J. Shin, M.M. Tajrishi, Y. Ogura, A. Kumar, Wasting mechanisms in muscular dystrophy, Int. J. Biochem. Cell Biol. 45 (2013) 2266–2279.
[55] A.J. Groen, K.S. Lilley, Proteomics of total membranes and subcellular membranes, Expert Rev. Proteomics 7 (2010) 867–878.
[56] K. Ohlendieck, Organelle proteomics in skeletal muscle biology, J. Integr. Omics. 2 (2012) 27–38.
[57] R. Drissi, M.L. Dubois, F.M. Boisvert, Proteomics methods for subcellular proteome analysis, FEBS J. 280 (2013) 5626–5634.
[58] M. Kaakinen, T. Kaisto, P. Rahkila, K. Metsikkö, Caveolin 3, flotillin 1 and influenza virus hemagglutinin reside in distinct domains on the sarcolemma of skeletal myofibers, Biochem. Res. Int. 2012 (2012) 497572.
[59] J.E. Bouameur, T.M. Magin, Lessons from animal models of cytoplasmic intermediate filament proteins, Subcell. Biochem. 82 (2017) 171–230.
[60] D.L. Sherman, L.M. Wu, M. Grove, C.S. Gillespie, P.J. Brophy, Drp2 and periaxin form Cajal bands with dystroglycan but have distinct roles in Schwann cell growth, J. Neurosci. 32 (2012) 9419–9428.
[61] S.J. Pratt, A.P. Valencia, G.K. Le, S.B. Shah, R.M. Lovering, Pre- and postsynaptic changes in the neuromuscular junction in dystrophic mice, Front. Physiol. 6 (2015) 252.
[62] S.E. Moore, F.S. Walsh, Nerve dependent regulation of neural cell adhesion molecule expression in skeletal muscle, Neuroscience 18 (1986) 499–505.
[63] G. Gosztonyi, U. Naschold, Z. Grozdanovic, G. Stoltenburg-Didinger, R. Gossrau, Expression of Leu-19 (CD56, N-CAM) and nitric oxide synthase (NOS) I in denervated and reinnervated human skeletal muscle, Microsc. Res. Tech. 55 (2001) 187–197.
[64] S.M. Prattis, S.B. Horton, S.D. van Camp, J.N. Kornegay, Immunohistochemical detection of neural cell adhesion molecule and laminin in X-linked dystrophic dogs and mdx mice, J. Comp. Pathol. 110 (1994) 253–266.
[65] Z. Horne, J. Hesketh, Immunological localization of ribosomes in striated rat muscle. Evidence for myofibrillar association and ontological changes in the subsarcolemmal:myofibrillar distribution, Biochem. J. 268 (1990) 231–236.
[66] N.J. Lennon, A. Kho, B.J. Bacskai, S.L. Perlmutter, B.T. Hyman, R.H. Brown Jr., Dysferlin interacts with annexins A1 and A2 and mediates sarcolemmal wound-healing, J. Biol. Chem. 278 (2003) 50466–50473.
[67] R. Han, K.P. Campbell, Dysferlin and muscle membrane repair, Curr. Opin. Cell Biol. 19 (2007) 409–416.
[68] A.R. Demonbreun, M. Quattrocelli, D.Y. Barefield, M.V. Allen, K.E. Swanson, E.M. McNally, An actin-dependent annexin complex mediates plasma membrane repair in muscle, J. Cell Biol. 213 (2016) 705–718.
[69] A.R. Demonbreun, A.E. Rossi, M.G. Alvarez, K.E. Swanson, H.K. Deveaux, J.U. Earley, M. Hadhazy, R. Vohra, G.A. Walter, P. Pytel, E.M. McNally, Dysferlin and myoferlin regulate transverse tubule formation and glycerol sensitivity, Am. J. Pathol. 184 (2014) 248–259.
[70] J.P. Kerr, C.W. Ward, R.J. Bloch, Dysferlin at transverse tubules regulates Ca^{2+} homeostasis in skeletal muscle, Front. Physiol. 5 (2014) 89.
[71] T.L. Boye, J. Nylandsted, Annexins in plasma membrane repair, Biol. Chem. 397 (2016) 961–969.
[72] D.B. Davis, A.J. Delmonte, C.T. Ly, E.M. McNally, Myoferlin, a candidate gene and potential modifier of muscular dystrophy, Hum. Mol. Genet. 9 (2000) 217–226.
[73] A. Vontzalidis, G. Terzis, P. Manta, Increased dysferlin expression in Duchenne muscular dystrophy, Anal. Quant. Cytol. Histol. 36 (2014) 15–22.
[74] V. Bizzarro, A. Petrella, L. Parente, Annexin A1: novel roles in skeletal muscle biology, J. Cell. Physiol. 227 (2012) 3007–3015.
[75] M.A. Sugimoto, J.P. Vago, M.M. Teixeira, L.P. Sousa, Annexin A1 and the resolution of inflammation: modulation of neutrophil recruitment, apoptosis, and clearance, J Immunol Res 2016 (2016) 8239258.
[76] K.R. Acharya, S.J. Ackerman, Eosinophil granule proteins: form and function, J. Biol. Chem. 289 (2014) 17406–17415.
[77] M. Nagappa, A. Nalini, G. Narayanappa, Major histocompatibility complex and inflammatory cell subtype expression in inflammatory myopathies and muscular dystrophies, Neurol. India 61 (2013) 614–621.
[78] T. Mustelin, K. Taskén, Positive and negative regulation of T-cell activation through kinases and phosphatases, Biochem. J. 371 (2003) 15–27.
[79] Woo HN1, G.S. Hong, J.I. Jun, D.H. Cho, H.W. Choi, H.J. Lee, C.W. Chung, I.K. Kim, D.G. Jo, J.O. Pyo, J. Bertin, Y.K. Jung, Inhibition of Bcl10-mediated activation of NF-kappa B by BinCARD, a Bcl10-interacting CARD protein, FEBS Lett. 578 (2004) 239–244.
[80] M.J. Spencer, J.G. Tidball, Do immune cells promote the pathology of dystrophin-deficient myopathies? Neuromuscul. Disord. 11 (2001) 556–564.
[81] B. De Paepe, J.L. De Bleecker, Cytokines and chemokines as regulators of skeletal muscle inflammation: presenting the case of Duchenne muscular dystrophy, Mediat. Inflamm. 2013 (2013) 540370.
[82] K. Mojumdar, F. Liang, C. Giordano, C. Lemaire, G. Danialou, T. Okazaki, J. Bourdon, M. Rafei, J. Galipeau, M. Divangahi, B.J. Petrof, Inflammatory monocytes promote progression of Duchenne muscular dystrophy and can be therapeutically targeted via CCR2, EMBO Mol. Med. 6 (2014) 1476–1492.
[83] A.S. Rosenberg, M. Puig, K. Nagaraju, E.P. Hoffman, S.A. Villalta, V.A. Rao, L.M. Wakefield, J. Woodcock, Immune-mediated pathology in Duchenne muscular dystrophy, Sci. Transl. Med. 7 (2015) 299rv4.
[84] S.A. Villalta, W. Rosenthal, L. Martinez, A. Kaur, T. Sparwasser, J.G. Tidball, M. Margeta, M.J. Spencer, J.A. Bluestone, Regulatory T cells suppress muscle inflammation and injury in muscular dystrophy, Sci. Transl. Med. 6 (2014) 258ra142.
[85] H.A. John, I.F. Purdom, Elevated plasma levels of haptoglobin in Duchenne muscular dystrophy: electrophoretic variants in patients with a severe form of the disease, Electrophoresis 10 (1989) 489–493.
[86] S.A. Villalta, A.S. Rosenberg, J.A. Bluestone, The immune system in Duchenne muscular dystrophy: friend or foe, Rare Dis. 3 (2015) e1010966.
[87] D. Gardan-Salmon, J.M. Dixon, S.M. Lonergan, J.T. Selsby, Proteomic assessment of the acute phase of dystrophin deficiency in mdx mice, Eur. J. Appl. Physiol. 111 (2011) 2763–2773.
[88] H. Brinkmeier, K. Ohlendieck, Chaperoning heat shock proteins: proteomic analysis and relevance for normal and dystrophin-deficient muscle, Proteomics Clin. Appl. 8 (2014) 875–895.
[89] P. Dowling, S. Murphy, K. Ohlendieck, Proteomic profiling of muscle fibre type shifting in neuromuscular diseases, Expert Rev. Proteomics 13 (2016) 783–799.
[90] C. Webster, L. Silberstein, A.P. Hays, H.M. Blau, Fast muscle fibers are preferentially affected in Duchenne muscular dystrophy, Cell 52 (1988) 503–513.
[91] J.F. Marini, F. Pons, J. Leger, N. Loffreda, M. Anoal, M. Chevallay, M. Fardeau, J.J. Leger, Expression of myosin heavy chain isoforms in Duchenne muscular dystrophy patients and carriers, Neuromuscul. Disord. 1 (1991) 397–409.
[92] P. Doran, S.D. Wilton, S. Fletcher, K. Ohlendieck, Proteomic profiling of antisense-induced exon skipping reveals reversal of pathobiochemical abnormalities in dystrophic mdx diaphragm, Proteomics 9 (2009) 671–685.
[93] L. Guevel, J.R. Lavoie, C. Perez-Iratxeta, K. Rouger, L. Dubreil, M. Feron, S. Talon, M. Brand, L.A. Megeney, Quantitative proteomic analysis of dystrophic dog muscle, J. Proteome Res. 10 (2011) 2465–2478.
[94] A. Holland, K. Ohlendieck, Proteomic profiling of the contractile apparatus from skeletal muscle, Expert Rev. Proteomics 10 (2013) 239–257.
[95] K. Ohlendieck, Proteomics of skeletal muscle glycolysis, Biochim. Biophys. Acta 1804 (2010) 2089–2101.
[96] P. Doran, P. Dowling, J. Lohan, K. McDonnell, S. Poetsch, K. Ohlendieck, Subproteomics analysis of Ca+-binding proteins demonstrates decreased calsequestrin expression in dystrophic mouse skeletal muscle, Eur. J. Biochem. 271 (2004) 3943–3952.
[97] P. Dowling, P. Doran, K. Ohlendieck, Drastic reduction of sarcalumenin in Dp427 (dystrophin of 427 kDa)-deficient fibres indicates that abnormal calcium handling

plays a key role in muscular dystrophy, Biochem. J. 379 (2004) 479–488.
[98] J.F. Dunn, K.A. Burton, M.J. Dauncey, Ouabain sensitive Na+/K+-ATPase content is elevated in mdx mice: implications for the regulation of ions in dystrophic muscle, J. Neurol. Sci. 133 (1995) 11–15.
[99] K. Ohlendieck, D. Swandulla, Molecular pathogenesis of Duchenne muscular dystrophy-related fibrosis, Pathologe 38 (2017) 21–29.
[100] S. Carberry, M. Zweyer, D. Swandulla, K. Ohlendieck, Proteomics reveals drastic increase of extracellular matrix proteins collagen and dermatopontin in the aged mdx diaphragm model of Duchenne muscular dystrophy, Int. J. Mol. Med. 30 (2012) 229–234.
[101] S. Ito, K. Nagata, Biology of Hsp47 (Serpin H1), a collagen-specific molecular chaperone, Semin. Cell Dev. Biol. 62 (2017) 142–151.